arXiv:2106.10022v2 [cs.LG] 23 Sep 2022

Local AdaGrad-Type Algorithm for Stochastic Convex-Concave Optimization

Luofeng Liao[1,2], Li Shen[2*], Jia Duan[2], Mladen Kolar[3] and Dacheng Tao[2]

[1]IEOR, Columbia Unviersity, NY, USA.
[2]JD Explore Academy, JD.com Inc, Beijing, China.
[3]Booth School of Business, University of Chicago, IL, USA.

*Corresponding author(s). E-mail(s): mathshenli@gmail.com;
Contributing authors: ll3530@columbia.edu; xuelandj@gmail.com;
mkolar@chicagobooth.edu; dacheng.tao@gmail.com;

Abstract

Large scale convex-concave minimax problems arise in numerous applications, including game theory, robust training, and training of generative adversarial networks. Despite their wide applicability, solving such problems efficiently and effectively is challenging in the presence of large amounts of data using existing stochastic minimax methods. We study a class of stochastic minimax methods and develop a communication-efficient distributed stochastic extragradient algorithm, LocalAdaSEG, with an adaptive learning rate suitable for solving convex-concave minimax problems in the Parameter-Server model. LocalAdaSEG has three main features: (i) a periodic communication strategy that reduces the communication cost between workers and the server; (ii) an adaptive learning rate that is computed locally and allows for tuning-free implementation; and (iii) theoretically, a nearly linear speed-up with respect to the dominant variance term, arising from the estimation of the stochastic gradient, is proven in both the smooth and nonsmooth convex-concave settings. LocalAdaSEG is used to solve a stochastic bilinear game, and train a generative adversarial network. We compare LocalAdaSEG against several existing optimizers for minimax problems and demonstrate its efficacy through several experiments in both homogeneous and heterogeneous settings.

Keywords: Stochastic Minimax Problem, Adaptive Optimization, Distributed Computation

1 Introduction

Stochastic minimax optimization problems arise in applications ranging from game theory [47], robust optimization [20], and AUC Maximization [29], to adversarial learning [53] and training of generative adversarial networks (GANs) [28]. In this work, we consider

$$\min_{x\in\mathcal{X}}\max_{y\in\mathcal{Y}}\left\{F(x,y)=\int_{\Xi}f(x,y,\xi)P(\mathrm{d}\xi)\right\}, \tag{1}$$

where $\mathcal{X}\subseteq\mathbb{X}$, $\mathcal{Y}\subseteq\mathbb{Y}$ are nonempty compact convex sets, $\mathbb{X}$, $\mathbb{Y}$ are finite dimensional vector spaces, ξ is a random vector with an unknown probability distribution P supported on a set Ξ, and $f:\mathcal{X}\times\mathcal{Y}\times\Xi\to\mathbb{R}$ is a real valued function, which may be nonsmooth. Throughout the paper, we assume that the expectation $\mathbb{E}_{\xi\sim P}[f(x,y,\xi)]$ is well defined and finite. For all $\xi\in\Xi$, we assume that the function $F(x,y)$ is convex in $x\in\mathcal{X}$ and concave in $y\in\mathcal{Y}$. In addition, we assume that $F(x,y)$ is a Lipschitz continuous function.

There are **three main challenges** in developing an efficient solver for the large-scale minimax problem (1). First, the solver should generate converging iterates. In contrast to convex optimization, convergence results for minimax problems are harder to obtain. Second, the solver should be able to take advantage of parallel computing in a communication-efficient way. Only then can it be applied to problems with large-scale datasets, which are often distributed across multiple workers. Third, it is desirable for the solver to choose learning rates in an adaptive manner. It is well known that, in minimax problems, solver performance is susceptible to learning rates. We discuss these challenges in detail below.

First, it has been shown that direct application of the (stochastic) gradient descent ascent ((S)GDA) to solve (1) may result in divergence of the iterates [42, 19, 27, 43]. Possible ways to overcome the divergence issue are to apply the primal-dual hybrid gradient (PDHG) or (stochastic) extragradient method and their variants [42, 19, 26, 4, 39, 58, 57].

Second, it is often desirable to have a communication-efficient distributed solver to solve the stochastic minimax problem (1). The first reason being that the minimax problem (1) is often instantiated as a finite-sum problem with large-scale datasets (with the distribution P being the empirical distribution over millions of data points), and thus storing and manipulating datasets on multiple workers is a must. For example, when problem (1) is specified as BigGAN [8] over ImageNet [21], the number of training samples is as many as 14 million. Traditional distributed SGDA on the problem (1) may suffer from a considerable communication burden; reducing communication complexity of the algorithm is a major concern in our paper. The second reason is that, in some scenarios, data are distributed on mobile devices (such as cell phones or smart watches), and due to privacy concerns, local data must stay on the device. Furthermore, frequent communication among devices is not feasible due to failures of mobile devices (network connectivity, battery

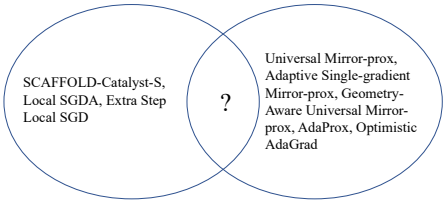


Fig. 1 A Venn Diagram for related works. Left circle: Communication-efficient methods for stochastic minimax problems. Right circle: Adaptive methods for stochastic minimax problems.

level, etc.). This further motivates the design of communication-efficient distributed solvers to eliminate central data storage and improve communication efficiency. For these reasons, communication-efficient distributed solvers for minimax problems have been investigated recently [7, 23, 31, 40].

Third, the performance of stochastic minimax solvers for (1) is highly dependent on the learning rate tuning mechanism [30, 1]. And yet, designing a solver for (1) with an adaptive learning rate is much more challenging compared to the convex case; the value of F at an iterate (x, y) does *not* serve as a performance criterion. For example, for classical minimization problems, the learning rate can be tuned based on the loss evaluated at the current iterate, which directly quantifies how close the iterate is to the minimum. However, such an approach does not extend to minimax problems and, therefore, a more sophisticated approach is required for tuning the learning rate. Development of adaptive learning rate tuning mechanisms for large scale stochastic minimax problems has been explored only recently [6, 5, 25, 1, 39]. Hence, we ask

Can we develop an efficient algorithm for the stochastic minimax problem (1) that enjoys convergence guarantees, communication-efficiency and adaptivity ***simultaneously****?*

We provide an affirmative answer to this question and develop LocalAdaSEG (Local Adaptive Stochastic Extragradient) algorithm. Our contributions are three-fold:

Novel communication-efficient distributed minimax algorithm. Fig. 1 illustrates the difference between LocalAdaSEG algorithm and the existing works. LocalAdaSEG falls under the umbrella of the Parameter-Server model [51] and adopts a periodic communication mechanism to reduce the communication cost between the server and the workers, similar to Local SGD/FedAvg [56, 52, 36] in federated learning [41]. In addition, in each worker, a local stochastic extragradient algorithm with an adaptive learning rate is performed independently with multiple iterations. Every once in a while, current iterates and adaptive learning rates from all workers are sent to the server. The server computes a weighted average of the iterates, where the weights are constructed from the received local adaptive learning rates. We emphasize that adaptive learning in each worker is distinct from others

and is automatically updated according to local data as is done in [11, 7], and different from the existing adaptive distributed algorithms [54, 48, 13].

Theoretically optimal convergence rate. Let M denote the number of workers, σ denote the variance of stochastic gradients, and T denote the number of local iterations on each worker. For stochastic convex-concave minimax problems, we establish the rate in terms of the duality gap metric [45, 37] as $\tilde{O}(\sigma/\sqrt{MT})$ in the *nonsmooth and noise-dominant* case and the rate $\tilde{O}(\sigma/\sqrt{MT} +$ higher-order terms) in *smooth case with slow cumulative gradient growth*. The terms depending on the variance σ achieve the statistical lower bound and are not improvable without further assumptions. Therefore, the LocalAdaSEG algorithm enjoys the linear speed-up property in the stochastic gradient variance term due to the periodic communication mechanism.

Experimental verification. We conduct several experiments on the stochastic bilinear game and the Wasserstein GAN [3] to verify the efficiency and effectiveness of the LocalAdaSEG algorithm. We also extend the LocalAdaSEG algorithm to solve the challenging federated GANs in a heterogeneous setting. The experimental results agree with the theoretical guarantees and demonstrate the superiority of LocalAdaSEG against several existing minimax optimizers, such as SEGDA [45], UMP [6], ASMP [25], LocalSEGDA [7], LocalSGDA [23], and Local Adam [7].

2 Related Work

Although there has been a lot of work on minimax optimization, due to space constraints, we summarize only the most closely related work. Our work is related to the literature on stochastic minimax algorithms, adaptive minimax algorithms, and distributed minimax algorithms. We defer a detailed discussion of related work to Section A in the appendix.

Our work and the proposed LocalAdaSEG contribute to the literature described above. To our knowledge, the proposed LocalAdaSEG algorithm is the first distributed communication-efficient algorithm for the stochastic minimax problem and simultaneously supports the adaptive learning rate and minibatch size. Moreover, LocalAdaSEG communicates only periodically to improve communication efficiency and uses a local adaptive learning rate, computed on local data in each worker, to improve the efficiency of computation. In addition, LocalAdaSEG can also be applied in a non-smooth setting with the convergence guarantee. LocalAdaSEG can be seen as a distributed extension of [6] with period communication as local SGD [52]. We note that only very recently a local adaptive stochastic minimax algorithm, called Local Adam, has been used heuristically to train GANs without a convergence guarantee [7]. We summarize the relationship with the existing literature in Table 1.

Stochastic minimax algorithms	Nonsmooth ?	Comm. eff. ?	Adaptive ?
Mirror SA [46], SMP [33], SAMP [17], Optimal Stochastic PDHG-type [58]	✓	✗	✗
SCAFFOLD-Catalyst-S [31], Local SGDA [23], Extra Step Local SGD [7]	✗	✓	✗
Universal Mirror-prox [6], Adaptive Single-gradient Mirror-prox [25], Geometry-Aware Universal Mirror-prox [5], AdaProx [1]	✓	✗	✓
Optimistic AdaGrad [39]	✗*	✗	✓
Our LocalAdaSEG	✓	✓	✓

Table 1 Comparison to related works on adaptive or communication-efficient approaches to stochastic minimax problems. Here "Nonsmooth ?" asks whether the algorithm enjoys theoretical guarantees in the nonsmooth convex-concave setting; "Comm. eff. ?" asks whether the proposed algorithm is communication-efficient; "Adaptive ?" asks whether the proposed algorithm requires knowledge of problem parameters. "*": The work of [39] discusses non-convex non-concave minimax problems.

3 Methodology

3.1 Notations and Assumptions

A point $(x^*, y^*) \in \mathcal{X} \times \mathcal{Y}$ is called a saddle-point for the minimax problem in (1) if for all $(x, y) \in \mathcal{X} \times \mathcal{Y}$,

$$F(x^*, y) \leq F(x^*, y^*) \leq F(x, y^*). \tag{2}$$

Under the assumptions stated in Section 1, the corresponding primal, $\min_x\{\max_y F(x, y)\}$, and dual problem, $\max_y\{\min_x F(x, y)\}$, have optimal solutions and equal optimal values, denoted F^*. The pairs of optimal solutions (x^*, y^*) form the set of saddle-points of F on $\mathcal{X} \times \mathcal{Y}$. We denote $\mathbb{Z} = \mathbb{X} \times \mathbb{Y}$, $\mathcal{Z} = \mathcal{X} \times \mathcal{Y}$, $z = (x, y) \in \mathcal{Z}$, and $z^* = (x^*, y^*) \in \mathcal{Z}$. We use $\|\cdot\|_{\mathcal{X}}$, $\|\cdot\|_{\mathcal{Y}}$, and $\|\cdot\|_{\mathcal{Z}}$ to denote the Euclidean norms on $\mathbb{X}$, $\mathbb{Y}$, $\mathbb{Z}$, respectively, and let $\|\cdot\|_{\mathcal{X},*}$, $\|\cdot\|_{\mathcal{Y},*}$ and $\|\cdot\|_{\mathcal{Z},*}$ denote the corresponding dual norms. With this notation, $\|z\|_{\mathcal{Z}} = \sqrt{\|x\|_{\mathcal{X}}^2 + \|y\|_{\mathcal{Y}}^2}$ and $\|z\|_{\mathcal{Z},*} = \sqrt{\|x\|_{\mathcal{X},*}^2 + \|y\|_{\mathcal{Y},*}^2}$. Throughout the paper, we focus on the Euclidean setting, but note that the results can readily generalize to non-Euclidean cases.

We are interested in finding a saddle-point of F over $\mathcal{X} \times \mathcal{Y}$. For a candidate solution $\tilde{z} = (\tilde{x}, \tilde{y}) \in \mathcal{Z}$, we measure its quality by the duality gap, defined as

$$\text{DualGap}(\tilde{z}) := \max_{y \in \mathcal{Y}} F(\tilde{x}, y) - \min_{x \in \mathcal{X}} F(x, \tilde{y}). \tag{3}$$

The duality gap is commonly used as a performance criterion for general convex-concave minimax problems (see, e.g., [45, 37]). Note that for all $z \in \mathcal{Z}$ it holds $\text{DualGap}(z) \geq 0$ and $\text{DualGap}(z) = 0$ if and only if z is a saddle-point.

For the stochastic minimax problem (1), we assume that neither the function $F(x, y)$ nor its sub/supgradients in x and y are available. Instead, we assume access to an unbiased stochastic oracle $G(x, y, \xi) = [G_x(x, y, \xi), -G_y(x, y, \xi)]$, such that the vector $\mathbb{E}_\xi[G(x, y, \xi)]$ is well-defined and $\mathbb{E}_\xi[G(x, y, \xi)] \in [\partial_x F(x, y), -\partial_y F(x, y)]$. For notational convenience, we let

$$\tilde{G}(z) := G(x, y, \xi), \quad G(z) := \mathbb{E}_\xi[G(x, y, \xi)]. \tag{4}$$

Below, we impose assumptions on the minimax problem (1) and the stochastic gradient oracle (4).

Assumption 1 (Bounded Domain) There exists D such that $\sup_{z \in \mathcal{Z}} \frac{1}{2}\|z\|^2 \leq D^2$.

Assumption 2 (Bounded Stochastic Gradients) There exists G such that $\sup_{z \in \mathcal{Z}} \|\tilde{G}(z)\|_* \leq G$, P-almost surely.

Domain boundedness Assumption 1 is commonly assumed in the convex-concave minimax literature; see references in Section 1. However, we note that the assumption might be removed in certain settings. For example, [16, 44] use a perturbation-based variant of the duality gap as the convergence criterion, and [1] handles unbounded domains via the notion of local norms, while [58] handles unbounded domains with access to a convex optimization oracle. The almost sure boundedness Assumption 2 on the gradient oracle seems restrictive but is common in the literature on adaptive stochastic gradient methods (see, e.g., [24, 14, 6, 39]). In Remark 2 we discuss how to extend our analysis to unbounded oracles.

Assumption 3 (Bounded Variance) There exists σ such that $\mathbb{E}_\xi\left[\|G(z) - \tilde{G}(z)\|_*^2 \,|\, z\right] \leq \sigma^2$ for P-almost every z.

We separately analyze the case when the saddle function F is differentiable with Lipschitz gradients.

Assumption 4 (Smoothness) Assume that for all $z, z' \in \mathcal{Z}$, we have $\|G(z) - G(z')\|_* \leq L\|z - z'\|$.

3.2 LocalAdaSEG Algorithm

We introduce the LocalAdaSEG algorithm used to solve (1) and describe its main features. Algorithm 1 details the procedure.

Algorithm 1 LocalAdaSEG($G_0, D;\ K, M, R;\ \alpha$)

1: **Input**: G_0, a guess on the upper bound of gradients, D, the diameter of the set $\mathcal{Z}$, K, communication interval, M, the number of workers, R, number of rounds, α, base learning rate.
2: **Initialize**: $\eta_1^m = D\alpha/G_0$, $\tilde{z}_0 = \tilde{z}_0^m = \tilde{z}_0^{m,*} = 0$ for all m, and $S := \{0, K, 2K, \dots, RK\}$.
3: **for** $t = 1, \dots, T = RK$, parallel for workers $m = 1, \dots, M$ **do**
4: update learning rate $\eta_t^m =$

$$D\alpha \Big/ \sqrt{G_0^2 + \sum_{\tau=1}^{t-1} \frac{\|z_\tau^m - \tilde{z}_{\tau-1}^{m,*}\|^2 + \|z_\tau^m - \tilde{z}_\tau^m\|^2}{5(\eta_\tau^m)^2}}$$

5: **if** $t - 1 \in S$ **then**
6: worker m: send $(\eta_t^m, \tilde{z}_{t-1}^m)$ to server
7: server: compute $\tilde{z}_{t-1}^\circ$, the weighted average of $\{\tilde{z}_{t-1}^m\}_{m\in[M]}$, and broadcast it to workers

$$w_t^m = \frac{(\eta_t^m)^{-1}}{\sum_{m'=1}^M (\eta_t^{m'})^{-1}},\ \tilde{z}_{t-1}^\circ = \sum_{m=1}^M w_t^m \cdot \tilde{z}_{t-1}^m$$

8: worker m: set $\tilde{z}_{t-1}^{m,*} = \tilde{z}_{t-1}^\circ$
9: **else**
10: set $\tilde{z}_{t-1}^{m,*} = \tilde{z}_{t-1}^m$
11: **end if**
12: update

$$z_t^m = \Pi_{\mathcal{Z}}[\tilde{z}_{t-1}^{m,*} - \eta_t^m M_t^m] \quad \text{with } M_t^m = \tilde{G}(\tilde{z}_{t-1}^{m,*})$$
$$\tilde{z}_t^m = \Pi_{\mathcal{Z}}[\tilde{z}_{t-1}^{m,*} - \eta_t^m g_t^m] \quad \text{with } g_t^m = \tilde{G}(z_t^m)$$

13: **end for**
14: **Output**: $\frac{1}{TM}\sum_{m=1}^M \sum_{t=1}^T z_t^m$

The Parameter-Server model. LocalAdaSEG uses M parallel workers which, in each of R rounds, independently execute K steps of extragradient updates (Line 12). The adaptive learning rate is computed solely based on iterates occurred in the local worker (Line 4). Let $S := \{0, K, 2K, \dots, RK = T\}$ denote the time points of communication. At a time of communication ($t \in S+1$, Lines 5–8), the workers communicate and compute the weighted iterate, $\tilde{z}_{t-1}^\circ$, defined in Line 7. Then the next round begins with a common iterate $\tilde{z}_{t-1}^\circ$. Finally, LocalAdaSEG outputs the average of the sequence $\{z_t^m\}_{m\in[M],t\in[T]}$. Overall, each worker computes $T = KR$ extragradient steps locally, for a

total of $2MT$ stochastic gradient calls (since each extragradient step, Line 12, requires two calls of gradient oracle) with R rounds of communication (every K steps of computation).

Extragradient step. At the time when no communication happens ($t-1 \notin S$), Line 12 reduces to

$$z_t^m = \Pi_{\mathcal{Z}}[\tilde{z}_{t-1}^m - \eta_t^m M_t^m] \qquad \text{with } M_t^m = \tilde{G}(\tilde{z}_{t-1}^m),$$
$$\tilde{z}_t^m = \Pi_{\mathcal{Z}}[\tilde{z}_{t-1}^m - \eta_t^m g_t^m] \qquad \text{with } g_t^m = \tilde{G}(z_t^m),$$

where $\Pi_{\mathcal{Z}}(z) = \operatorname{argmin}_{z' \in \mathcal{Z}} \|z - z'\|_2$ is the projection operator onto the compact set $\mathcal{Z}$. The above update is just the extragradient (EG) algorithm [35] that is commonly used to solve minimax problems; see references in Section 1.

Periodic averaging weights. The proposed weighted averaging scheme in Line 7 is different from existing works on local SGD and Local Adam [7]. At the time of averaging ($t-1 \in S$), LocalAdaSEG pulls the averaged iterate towards the local iterate with a smaller learning rate. For the homogeneous case studied in this paper, we expect $w^m \sim 1/M$.

Intuition of local adaptive learning rate scheme. The adaptive learning rate scheme (Line 4) follows that of Bach and Levy [6] closely. To develop intuition, consider the deterministic setting where $\sigma = 0$ and define $(\delta_t^m)^2 := \|g_t^m\|_*^2 + \|M_t^m\|_*^2$. If we ignore the projection operation, the learning rate η_t^m would look like $\eta_t^m \sim 1/(1 + \sum_{\tau=1}^{t-1} (\delta_\tau^m)^2)^{1/2}$. In the nonsmooth case, the subgradients might not vanish as we approach the solution (in the case of convex optimization, consider the function $f(x) = \mathsf{x}$ near 0), and we only have $\liminf_{t\to\infty} \delta_t^m > 0$. This implies η_t^m will vanish at the rate $1/\sqrt{t}$, which is the optimal learning rate scheme for nonsmooth convex-concave problems [6, 1]. For the smooth case, one might expect the sequence $\{\delta_t^m\}_t$ to be square-summable and $\eta_t^m \to \eta_\infty^m > 0$, in which case the learning rate does not vanish. Additionally, the adaptive learning rate for each worker is locally updated to exploit the problem structure available in worker's local dataset. This makes our local adaptive learning rate scheme distinct compared to existing distributed adaptive algorithms for minimization problems [54, 48, 13]. Very recently, [7] used local Adam for training conditional GANs efficiently, but they provide theoretical guarantees only for the local extragradient without adaptivity.

Adaptivity to (G, L, σ). Our algorithm does not require knowledge of problem parameters such as the size of the gradients G, the smoothness L, or the variance of gradient estimates σ. Instead, we only need an initial guess of G, denoted G_0, and the diameter of the feasible set, D. Following [6], we define

$$\gamma := \max\{G/G_0, G_0/G\} \geq 1. \tag{5}$$

This quantity measures how good our guess is and appears in the convergence guarantees for the algorithm. Our algorithm still requires knowledge of the

problem class, as we need to use a different base learning rate, α, for smooth and nonsmooth problems; see Theorems 1 and 2, respectively.

3.3 Convergence Results

We state two theorems characterizing the convergence rate of LocalAdaSEG for the smooth and nonsmooth problems. We use the notation $\tilde{O}$ to hide absolute constants and logarithmic factors of $T = KR$ and problem parameters. The proofs are given in Section C.1 and Section C.2 of the appendix. Recall the definition of γ in (5).

Theorem 1 (Nonsmooth Case) *Assume that Assumptions 1, 2, and 3 hold. Let* $\bar{z} = \text{LocalAdaSEG}(G_0, D;\ K, M, R;\ 1)$. *Then*

$$\mathbb{E}[\text{DualGap}(\bar{z})] = \tilde{O}\left(\frac{\gamma G D}{\sqrt{T}} + \frac{\sigma D}{\sqrt{MT}}\right).$$

Theorem 2 (Smooth Case) *Assume that Assumptions 1, 2, 3, and 4 hold. Let* $\bar{z} = \text{LocalAdaSEG}(G_0, D;\ K, M, R;\ 1/\sqrt{M})$. *Define the cumulative norms of stochastic gradients occurred on worker* m *as*

$$\mathcal{V}_m(T) := \mathbb{E}\left[\sqrt{\sum_{t=1}^{T} \|g_t^m\|_*^2 + \|M_t^m\|_*^2}\right]. \tag{6}$$

Then

$$\mathbb{E}[\text{DualGap}(\bar{z})] = \tilde{O}\left(\frac{\sigma D}{\sqrt{MT}} + \frac{D\sqrt{M}\mathcal{V}_1(T)}{T} + \frac{\gamma^2 L D^2 M^{-1/2}}{T} + \frac{\gamma G D\sqrt{M}}{T}\right). \tag{7}$$

Remark 1 (The term $\mathcal{V}_1(T)$.) Note that by symmetry $\mathcal{V}_m(T) = \mathcal{V}_1(T)$ for all m. Although a trivial bound on $\mathcal{V}_1(T)$ is $\mathcal{V}_1(T) \le G\sqrt{2T}$, typically we have $\mathcal{V}_1(T) \ll \sqrt{T}$ in practice [24, 49, 18, 14, 39], especially in the sparse data scenarios. For example, consider the bilinear saddle-point problem $\min_{x\in\mathcal{X}} \max_{y\in\mathcal{Y}} \{x^\top (\sum_{i=1}^n p_i M_i) y\}$, where a larger weight $p_i > 0$ means the matrix M_i appears more frequently in the dataset. When most of matrices with large weights are row-sparse and column-sparse, the quantity $\mathcal{V}_1(T)$ is much smaller than $G\sqrt{2T}$. Theorem 5, in the appendix, shows that with a different choice of the base learning rate α one can obtain a near linear speed-up result, which removes the dependence on $\mathcal{V}_1(T)$: for large T,

$$\mathbb{E}[\text{DualGap}(\bar{z})] = \tilde{O}\left(\frac{\sigma D}{\sqrt{MT^{1-2\epsilon}}} + \frac{\gamma^2 L D^2}{T^{1-2\epsilon}} + \frac{L D^2 M}{T} + \frac{\gamma G D M^{3/2}}{T^{1+\epsilon}}\right),$$

for any $\epsilon \in (0, \frac{1}{2})$. Following the discussion in [18, 39], when the cumulative growth of the stochastic gradient is slow, i.e., $\mathcal{V}_1(T) = O(T^b)$ for some $0 < b < \frac{1}{2}$, then the second term in (7) is $O(DM^{3/2}/T^{1-b})$ and linear speed-up is achieved, since as $T \to \infty$, the dominating term become $O(\sigma D/\sqrt{MT})$.

Remark 2 (Extension to unbounded stochastic gradient oracle) Our analysis can be extended to unbounded homogeneous and light-tailed oracles using the following argument. Let

$$\|G\|_\infty := \sup_{z\in\mathcal{Z}} \|G(z)\|_* < \infty,$$

which upper bounds the expectation of the SG oracle. Assume $\|\tilde{G}(z)-G(z)\|_*/\|G\|_\infty$ is independent of z and follows the distribution of the absolute value of a standard normal. Define the set $\mathcal{Z}' := \{z_t^m, \tilde{z}_{t-1}^{m,*}\}_{t,m}$ of all iterates. For any $0 < \delta < 1$, define the event

$$\mathcal{E} := \Big\{ \max_{z'\in\mathcal{Z}'} \|\tilde{G}(z') - G(z')\|_* \le G_{T,\delta} := \|G\|_\infty \cdot \big(\sqrt{2\log(4MT)} + \sqrt{2\log(2/\delta)}\big)\Big\}.$$

Then $\mathbb{P}(\mathcal{E}) \ge 1-\delta$; see Appendix B.1. We can repeat the proof of Theorem 1 and Theorem 2 on the event $\mathcal{E}$ and interpret our results with G replaced by $G_{T,\delta}$, which effectively substitutes G with $\|G\|_\infty$ at the cost of an extra $\log(T)$ factor.

Remark 3 (Baseline 1: Minibatch EG) We comment on the performance of an obvious baseline that implements minibatch stochastic EG using M workers. Suppose the algorithm takes R extragradient steps, with each step using a minibatch of size KM, resulting in a procedure that communicates exactly R times. The performance of such a minibatch EG for general nonsmooth and smooth minimax problems [6, 25] is, respectively,[1]

$$O\bigg(\frac{\sigma D}{\sqrt{KMR}} + \frac{\|G\|_\infty D}{\sqrt{R}}\bigg) \text{ and } O\bigg(\frac{\sigma D}{\sqrt{KMR}} + \frac{LD^2}{R}\bigg).$$

Under the same computation and communication structure, our algorithm enjoys adaptivity, achieves the same linear speed-up in the variance term $\frac{\sigma D}{\sqrt{KMR}}$, and improves dependence on the gradient upper bound $\|G\|_\infty$ and the smoothness parameter L, which is a desirable property for problems where these parameters are large.

Remark 4 (Baseline 2: EG on a single worker) Another natural baseline is to run EG on a single worker for T iterations with batch-size equal to one. The convergence rates for this procedure in nonsmooth and smooth cases are $O(\sigma D/\sqrt{T} + \|G\|_\infty D/\sqrt{T})$ and $O(\sigma D/\sqrt{T} + LD^2/T)$, respectively. In the smooth case, EG on a single worker is inferior to minibatch EG, since the dominant term for the former is $1/\sqrt{T}$, but it is $1/\sqrt{MT}$ for the latter. On the other hand, in the nonsmooth case, minibatch EG reduces the variance term, but the term involving the deterministic part degrades. Therefore, in the nonsmooth case, we can only claim that the minibatch EG is better than the single-worker mode in the noise-dominant regime $\sigma = \Omega(\|G\|_\infty\sqrt{M})$.

Remark 5 (On the choice of K) Consider the baseline minibatch EG (see Remark 3) which runs as follows: the algorithm takes R extragradient steps, with each step using a minibatch of size KM, resulting in a procedure that communicates exactly R times. Note this procedure has exactly the same computation and communication structure

[1] These bounds hold due to Theorem 4 of [25], whose rates for nonsmooth and smooth problems are of the form $O(R(G+\sigma)/\sqrt{T})$ and $O(\beta R^2/T + R\sigma/\sqrt{T})$, respectively. The claim follows with σ in the original theorem statement replaced by $\sigma/\sqrt{KM}$, β by L, R by D, G by $\|G\|_\infty$, and T by R.

as LocalAdaSEG, facilitating a fair comparison. In the non-smooth case, our theory shows that LocalAdaSEG dominates minibatch EG regardless of the choice K. Therefore, let us focus the discussion on the *smooth loss with slow gradient growth case*. Suppose that the gradient growth term $\mathcal{V}_m(T) := \mathbb{E}\big[(\sum_{t=1}^{T} \|g_t^m\|_*^2 + \|M_t^m\|_*^2)^{1/2}\big]$ admits a rate $\mathcal{V}_m(T) = O(T^b)$ for some $0 < b < 1/2$. Theorem 2 then shows that LocalAdaSEG enjoys a convergence rate (ignoring problem parameters L, D and G)

$$\frac{1}{\sqrt{MKR}} + \frac{\sqrt{M}}{(KR)^{1-b}} + \frac{\sqrt{M}}{KR} ,$$

where M is the number of machines, R the communication rounds, and K is the length between two communications. The minibatch EG attains the convergence rate

$$\frac{1}{\sqrt{MKR}} + \frac{1}{R} .$$

Both algorithms achieve linear speedup, i.e., the dominant term is $O(\sigma/\sqrt{MKR})$. In order for LocalAdaSEG to be comparable with minibatch EG in the higher order term, we set $\sqrt{M}/(KR)^{1-b} = \Theta(1/R)$ and $\sqrt{M}/(KR) = O(1/R)$ and obtain $K = \Theta(\sqrt{M}T^b)$. With this choice of K, LocalAdaSEG achieves a communication efficiency no worse than minibatch EG with the crucial advantage of being tuning-free. Compared with case of optimizing strongly-convex functions, local SGD needs $K = O(\sqrt{T})$ to achieve linear speedup [52]. The discussion here is purely theoretical, since the exponent of gradient growth b is hard to estimate in practice.

Proof Sketch of Theorem 2

We present a proof sketch for the smooth case. Recall the update formula

$$\begin{aligned} z_t^m &= \Pi_{\mathcal{Z}}[\tilde{z}_{t-1}^{m,*} - \eta_t^m M_t^m] && \text{with } M_t^m = \tilde{G}(\tilde{z}_{t-1}^{m,*}), \\ \tilde{z}_t^m &= \Pi_{\mathcal{Z}}[\tilde{z}_{t-1}^{m,*} - \eta_t^m g_t^m] && \text{with } g_t^m = \tilde{G}(z_t^m). \end{aligned}$$

Fig. 2 provides a computation diagram and illustrates the relationship between the above variables.

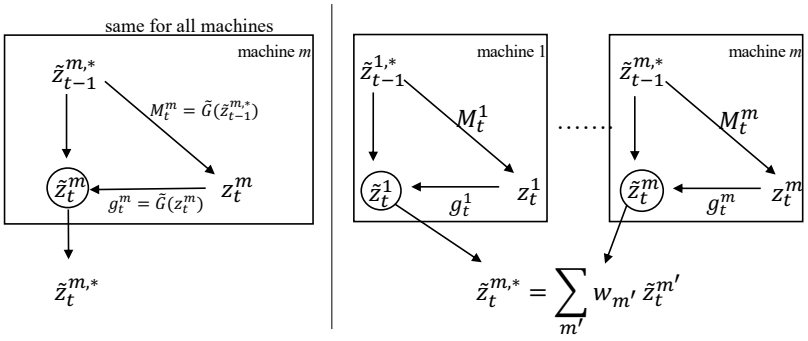


Fig. 2 The computation diagram for LocalAdaSEG. Left panel: computation on machine m when no communication ($t \notin S$). Right panel: computation on machine m when on communication round ($t \in S$)

We define the noise in the gradient operator G by

$$\xi_t^m := G(z_t^m) - g_t^m = G(z_t^m) - \tilde{G}(z_t^m).$$

Moreover, we define a gradient-like quantity

$$(Z_t^m)^2 := \frac{\left\|z_t^m - \tilde{z}_{t-1}^{m,*}\right\|^2 + \|z_t^m - \tilde{z}_t^m\|^2}{5\,(\eta_t^m)^2}.$$

If we ignore the projection operator in the update, the term (Z_t^m) will be of a similar scale as the gradients $\tilde{G}(z_t^m)$ and $\tilde{G}(\tilde{z}_t^m)$.

We begin with the following decomposition: for all $z \in \mathcal{Z}$,

$$\begin{aligned}
&\sum_{t=1}^{T}\sum_{m=1}^{M}\left\langle z_t^m - z, G(z_t^m)\right\rangle \\
&= \sum_{t=1}^{T}\sum_{m=1}^{M}\left\langle z_t^m - z, \xi_t^m\right\rangle + \sum_{t=1}^{T}\sum_{m=1}^{M}\langle z_t^m - z, g_t^m\rangle \\
&\le \underbrace{\sum_{t=1}^{T}\sum_{m=1}^{M}\left\langle z_t^m - z, \xi_t^m\right\rangle}_{I(z)} \\
&\quad + \underbrace{\sum_{t=1}^{T}\sum_{m=1}^{M}\frac{1}{\eta_t^m}\left(\tfrac{1}{2}\|z - \tilde{z}_{t-1}^{m,*}\|^2 - \tfrac{1}{2}\|z - \tilde{z}_t^m\|^2\right)}_{II(z)} \\
&\quad \underbrace{-\sum_{t=1}^{T}\sum_{m=1}^{M}\frac{1}{\eta_t^m}\left(\tfrac{1}{2}\|z_t^m - \tilde{z}_{t-1}^{m,*}\|^2 + \tfrac{1}{2}\|z_t^m - \tilde{z}_t^m\|^2\right)}_{III} \\
&\quad + \underbrace{\sum_{t=1}^{T}\sum_{m=1}^{M}\|g_t^m - M_t^m\|_* \cdot \|z_t^m - \tilde{z}_t^m\|}_{IV},
\end{aligned}$$

where we have used a descent lemma for EG updates common in the literature (Lemma 4 in our paper). The reason we care about the above quantity is that by the convexity-concavity of the problem, the duality gap metric can be upper-bounded by this term.

Next, we analyze each term separately. The term $I(z)$ characterizes the noise of the problem and eventually contributes to the noise term $\frac{\sigma}{\sqrt{KMR}}$. For the term II we use a telescoping argument and show that it can be upper bounded by $\sum_{m,t}\eta_t^m(Z_t^m)^2$. The telescoping argument can be applied due to the averaging weights w_t^m in the algorithm. The term III is negative. We keep the tail part of III which cancels the tail part of the term IV.

For the term IV we use the smoothness property of the problem and show that it can be bounded by $\sum_{m,t}(\eta_t^m)^2(Z_t^m)^2$. Finally, two sums of the form $\sum_{m,t}\eta_t^m(Z_t^m)^2$ and $\sum_{m,t}(\eta_t^m)^2(Z_t^m)^2$ remain to be handled. For this we use the well-known basic inequality $\sum_{i=1}^n a_i/(a_0+\sum_{j=1}^{i-1}a_j) = O(\log(1+\sum_i a_i))$ and $\sum_{i=1}^n a_i/\sqrt{a_0+\sum_{j=1}^{i-1}a_j} = \Theta(\sqrt{\sum_i a_i})$ for positive numbers a_i's.

Nonadaptive local algorithms rely on choosing a vanishing stepsize that is usually inversely proportional to a prespecified number of total iterations T. The freedom to choose the stepsize based on a prespecified T is crucial in the proofs of these algorithms and allows canceling of the asynchronicity of updates caused by local updates and the bias in those updates caused by data heterogeneity. This is the case for both convex optimization and convex-concave optimization. However, in the adaptive algorithm regimes, such a proof technique is clearly not viable.

Our algorithm requires a carefully designed iterates averaging scheme, with weight inversely proportional to stepsize. Such averaging-scheme is designed to account for the asynchronicity of local iterates and is automatically determined by the optimization process. This is what enables the extension of an Adam-type stepsize to parallel settings, which is highly nontrivial.

4 Experiments

We apply LocalAdaSEG to the stochastic bilinear minimax problem introduced in [26, 7] and train the Wasserstein generative adversarial neural network (Wasserstein GAN) [3]. For the homogeneous setting, to demonstrate the efficiency of our proposed algorithm, we compare LocalAdaSEG with minibatch stochastic extragradient gradient descent (MB-SEGDA) [45], minibatch universal mirror-prox (MB-UMP) [6], minibatch adaptive single-gradient mirror-Prox (MB-ASMP) [25], extra step local SGD (LocalSEGDA) [7], and local stochastic gradient descent ascent (LocalSGDA) [23]. We further extend the proposed LocalAdaSEG algorithm to solve federated WGANs with a heterogeneous dataset to verify its efficiency. To validate the practicality of LocalAdaSEG, we also train the BigGAN [8] over CIFAR10 dataset under the heterogeneous setting. In this setting, we also compare LocalAdaSEG with Local Adam [7]. We emphasize here that whether Local Adam converges is still an open question, even for the stochastic convex-concave setting.

4.1 Stochastic bilinear minimax problem

We consider the stochastic bilinear minimax problem with box constraints

$$\min_{x\in C^n}\max_{y\in C^n} F(x,y) \tag{8}$$

where

$$F(x,y) := \mathbb{E}_{\xi\sim P}\left[x^\top A y + (b+\xi)^\top x + (c+\xi)^\top y\right],$$

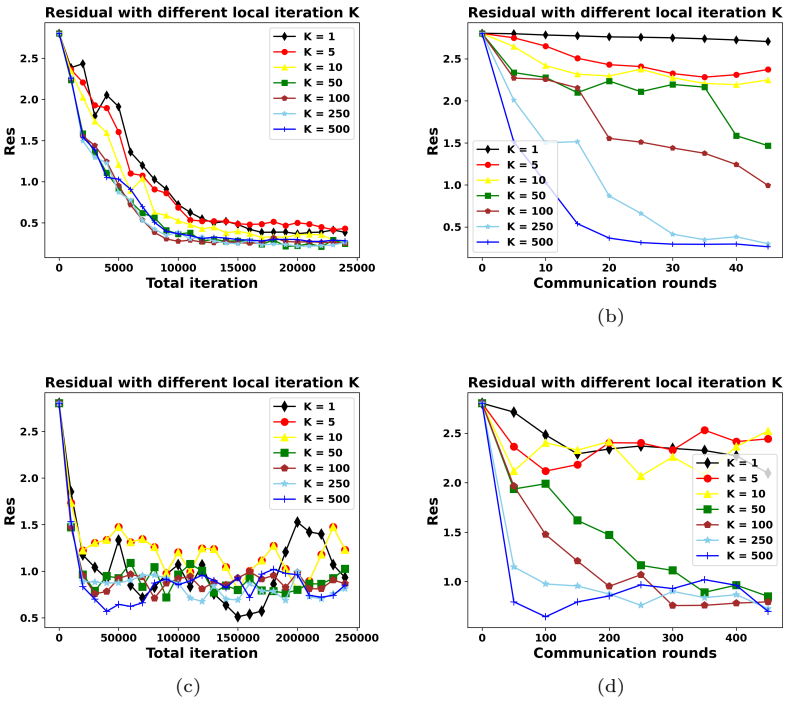


Fig. 3 Subfigures (a)-(b) and (c)-(d) plot the residual of LocalAdaSEG against the total number of iterations T and communications R, with varying numbers of local iterations K. We also investigate the effect of noise level ($\sigma = 0.1$ in (a)(b) and $\sigma = 0.5$ in (c)(d)).

Here $C^n = [-1, 1]^n$ is a box in $\mathbb{R}^n$, the tuple (A, b, c) is deterministic, and the perturbation variable ξ follows the normal distribution with variance σ. We define the KKT residual $\mathrm{Res}(x, y)$ as:

$$\begin{aligned}\mathrm{Res}(x,y)^2 :=& \|x - \Pi_{C^n}\big(x - (Ay + b)\big)\|^2 \\ &+ \|y - \Pi_{C^n}\big(y + (Ax + c)\big)\|^2.\end{aligned}$$

It is not hard to verify that given $(x^*, y^*) \in \mathbb{R}^n \times \mathbb{R}^n$, $\mathrm{Res}(x^*, y^*) = 0$ if and only if (x^*, y^*) belongs to the set of saddle-points of the bilinear minimax problem (8). During experiments, we use $\mathrm{Res}(x, y)$ to measure the quality of the approximate solution obtained by different optimizers.

Dataset Generation. We uniformly generate b and c in $[-1, 1]^n$ with $n = 10$. The symmetric matrix A is constructed as $A = \bar{A}/\max\big(\mathsf{b}_{\max}, \mathsf{c}_{\max}\big)$, where $\bar{A} \in [-1, 1]^{n\times n}$ is a random symmetric matrix. We emphasize that A is merely symmetric, but not semi-definite. To simulate the distributed environment, we distribute (A, b, c) to M workers, where $M = 4$. Each

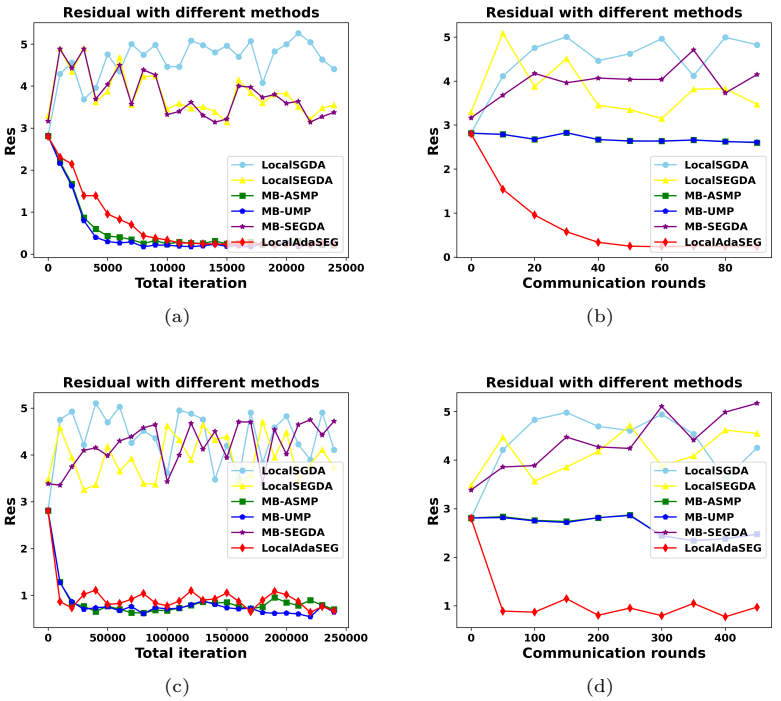


Fig. 4 Subfigures (a)-(b) and (c)-(d) compare LocalAdaSEG with existing optimizers. We plot the residuals against the total number of iterations T and communications R with different noise levels ($\sigma = 0.1$ in (a)(b) and $\sigma = 0.5$ in (c)(d)).

worker solves the above bilinear problem locally with an optimization algorithm. We instantiate LocalAdaSEG with different numbers of local iterations $K \in \{1, 5, 10, 50, 100, 250, 500\}$, and different noise levels $\sigma \in \{0.1, 0.5\}$, shown in Fig. 3. A larger σ indicates more noise in the stochastic gradients, making problem (8) harder. Furthermore, we compare LocalAdaSEG by setting the local iteration $K = 50$ against several existing optimizers, illustrated in Fig. 4.

Experimental Results. In Fig. 3, LocalAdaSEG provides stable convergence results under different configurations of local iterations K and noise levels σ. Figure (b)(d) illustrates that a suitably large K could accelerate the convergence speed of LocalAdaSEG. Figure (a)(c) illustrates that a large variance would result in unstable optimization trajectories. The findings of the experiment agree with our theoretical predictions: (i) a larger $T = KR$ improves convergence; (ii) the variance term dominates the convergence rate of LocalAdaSEG; a large variance term will slow down LocalAdaSEG. In Fig. 4, (a)(c) illustrate that adaptive variants of stochastic minimax optimizers, i.e., LocalAdaSEG, MB-UMP, and MB-ASMP, achieve better performance compared to standard ones such as LocalSGDA, LocalSEGDA, and MB-SEGDA, whose learning rates are hard to tune for minimax problems.

Furthermore, when compared in terms of communication rounds in (b)(d), LocalAdaSEG converges faster than other distributed stochastic minimax optimizers, demonstrating the superiority of LocalAdaSEG.

To validate the performance of our proposed method, we conduct the comparison of the asynchronous case and the synchronous case of LocalAdaSEG for the stochastic bilinear minimax problem. We also compare asynchronous and synchronous cases with the single-thread version (SEGDA with MKR iterations) from the aspects of residual and wallclock time. Finally, we evaluate the quantity of V_t with the update t. The experimental details are described in Appendix E.1. As can be seen in Fig. E1 (in Appendix E.1), compared with synchronous cases, asynchronicity only affects the convergence rate that is slower than the synchronous version with respect to the communication rounds. Compared to SEGDA of MKR iterations, our proposed LocalAdaSEG can achieve more stable and better performance. Regarding the quantity of Vt, it is really much smaller than the dominant variance term.

4.2 Wasserstein GAN

We train Wasserstein GAN (WGAN) to validate the efficiency of LocalAdaSEG on a real-world application task. This is a challenging minimax problem as the objectives of both generator and discriminator are non-convex and non-concave. The description of the problem and implementation details are placed in Section E.2.

Experimental results. Fig. E2 and E3 (in Section E.2) compare MB-UMP, MB-ASMP, LocalAdam and LocalAdaSEG in a homogeneous and heterogeneous setting, respectively. In Fig. E2(a) and Fig. E3(a), MB-UMP, MB-ASMP, LocalAdam and LocalAdaSEG quickly converge to a solution with a low FID value. However, when compared in terms of communication rounds in Fig. E2(b) and Fig. E3(b), LocalAdaSEG and Local Adam converge faster than other optimizers and reach a satisfactory solution in just a few rounds. In Fig. E2(c) and Fig. E3(c), all the listed optimizers achieve a high IS. In particular, the IS of LocalAdaSEG and Local Adam increases much faster with less communication than MB-UMP, MB-ASMP as shown in Fig. E2(d) and Fig. E3(d).

In Fig. E4 and Fig. E5, we show and compare the FID and IS of LocalAdaSEG with other optimizers under different data distributions. As can be seen from Fig. E4, LocalAdaSEG converges faster when the Dirichlet distribution parameter α decreases. In Fig. E5, when data distribution changes, our LocalAdaSEG can still converge faster than other existing optimizers.

4.3 BigGAN

To validate the practicability of our proposed LocalAdaSEG method, we apply LocaAdaSEG to train the large-scale BigGAN [8] model over the CIFAR10 dataset. The description of BigGAN and parameter setup are placed in *Section E.3*.

Experimental results. Fig. E6 illustrates the comparison of the FID and IS against communication rounds by using LocalAdaSEG and existing optimizers. As can be seen from Fig. E6(a), LocalAdaSEG and Local Adam can reach a satisfactory FID value in a few rounds. Similarly, from Fig. E6(b), we can see that the IS value of LocalAdaSEG and Local Adam is much higher than that of MB-UMP and MB-ASMP. In a word, the FID and IS values of LocalAdaSEG and Local Adam converge much faster than that of other optimizers.

Additional Discussions

To end this section, we briefly discuss the limitation of current work.

Theoretical limitations. Our theory is applicable to the homogeneous setting, meaning each worker has access to data from one distribution. However, in practice, data heterogeneity is a main factor practitioners must take into account for distributed learning. We briefly discuss technical challenges here. For the heterogeneous case, the theory for *non-adaptive* algorithms relies on choosing a very small stepsize, usually inverse proportional to a prespecified number of total iterations T. The freedom to choose the stepsize based on a prespecified T is crucial in those proofs and enables canceling the bias caused by local updates, a.k.a. client drifts. The same situation also occurs in the convex optimization case. However, our goal is to have an adaptive algorithm that does not depend on the problem parameters or a prespecified T. For this reason, we leave such an important open question for future work.

Experimental limitations. In the scale of the dataset, we experimented with should be increased to showcase the computation benefit of the proposed algorithm. At the current stage we have experimented with MNIST data and further, add CIFAR 10 experiments after reviewers' suggestions. Application to other ultra-large datasets such as ImageNet requires significant engineering efforts and will be left for future investigation. We should emphasize that our paper mainly contributes to the theoretical understanding of adaptive algorithms in distributed settings.

5 Conclusion

We proposed an adaptive communication-efficient distributed stochastic extragradient algorithm in the Parameter-Server model for stochastic convex-concave minimax problem, LocalAdaSEG. We theoretically showed LocalAdaSEG that achieves the optimal convergence rate with a linear speed-up property for both nonsmooth and smooth objectives. Experiments verify our theoretical results and demonstrate the efficiency of LocalAdaSEG.

For future work, since that the current analysis merely holds for the homogeneous setting, a promising direction is to extend the theoretical result of LocalAdaSEG to the heterogeneous setting that better models various real-world applications, such as federated GANs [7] and robust federated learning [22]. In addition, extending theoretical results from the stochastic

convex-concave setting to the stochastic nonconvex-(non)concave setting is an interesting and challenging research direction.

Declarations

- Funding (This work is supported by the Major Science and Technology Innovation 2030 "Brain Science and Brain-like Research" key project (No. 2021ZD0201405).)
- Conflict of interest/Competing interests (The authors declare that they have no conflict of interest.)
- Ethics approval (Not Applicable.)
- Consent to participate (Not Applicable.)
- Consent for publication (Not Applicable.)
- Availability of data and materials (The data used in this work is all public.)
- Code availability (The codes of the proposed method will be released after publishing.)
- Authors' contributions (All authors contributed to the study conception and design. The first draft of the manuscript was written by Luofeng Liao, and all authors commented on previous versions of the manuscript. All authors read and approved the final manuscript.)

If any of the sections are not relevant to your manuscript, please include the heading and write 'Not applicable' for that section.

Editorial Policies for:

Springer journals and proceedings:
https://www.springer.com/gp/editorial-policies

Nature Portfolio journals:
https://www.nature.com/nature-research/editorial-policies

Scientific Reports:
https://www.nature.com/srep/journal-policies/editorial-policies

BMC journals:
https://www.biomedcentral.com/getpublished/editorial-policies

References

[1] K. Antonakopoulos, V. Belmega, and P. Mertikopoulos. Adaptive extra-gradient methods for min-max optimization and games. In *International Conference on Learning Representations*, 2021.

[2] M. Arjovsky and L. Bottou. Towards principled methods for training generative adversarial networks. *arXiv preprint arXiv:1701.04862*, 2017.

[3] M. Arjovsky, S. Chintala, and L. Bottou. Wasserstein generative adversarial networks. In D. Precup and Y. W. Teh, editors, *Proceedings of the 34th International Conference on Machine Learning, ICML 2017, Sydney, NSW, Australia, 6-11 August 2017*, volume 70 of *Proceedings of Machine Learning Research*, pages 214–223. PMLR, 2017.

[4] W. Azizian, I. Mitliagkas, S. Lacoste-Julien, and G. Gidel. A tight and unified analysis of gradient-based methods for a whole spectrum of differentiable games. In *International Conference on Artificial Intelligence and Statistics*, pages 2863–2873. PMLR, 2020.

[5] R. Babanezhad and S. Lacoste-Julien. Geometry-aware universal mirror-prox. *arXiv preprint arXiv:2011.11203*, 2020.

[6] F. Bach and K. Y. Levy. A universal algorithm for variational inequalities adaptive to smoothness and noise. In *Conference on Learning Theory*, pages 164–194. PMLR, 2019.

[7] A. Beznosikov, V. Samokhin, and A. Gasnikov. Distributed saddle-point problems: Lower bounds, optimal algorithms and federated gans. *arXiv preprint arXiv:2010.13112*, 2021.

[8] A. Brock, J. Donahue, and K. Simonyan. Large scale gan training for high fidelity natural image synthesis. In *International Conference on Learning Representations*, 2019.

[9] A. Chambolle and T. Pock. A first-order primal-dual algorithm for convex problems with applications to imaging. *Journal of Mathematical Imaging and Vision*, 40(1):120–145, Dec. 2010.

[10] S. Chatterjee. *Superconcentration and Related Topics*. Springer International Publishing, 2014.

[11] C. Chen, L. Shen, H. Huang, and W. Liu. Quantized adam with error feedback. *ACM Transactions on Intelligent Systems and Technology (TIST)*, 12(5):1–26, 2021.

[12] C. Chen, L. Shen, F. Zou, and W. Liu. Towards practical adam: Non-convexity, convergence theory, and mini-batch acceleration. *arXiv preprint arXiv:2101.05471*, 2021.

[13] T. Chen, Z. Guo, Y. Sun, and W. Yin. Cada: Communication-adaptive distributed adam. In *International Conference on Artificial Intelligence and Statistics*, pages 613–621. PMLR, 2021.

[14] X. Chen, S. Liu, R. Sun, and M. Hong. On the convergence of a class of adam-type algorithms for non-convex optimization. In *International Conference on Learning Representations*, 2019.

[15] X. Chen, S. Yang, L. Shen, and X. Pang. A distributed training algorithm of generative adversarial networks with quantized gradients. *arXiv preprint arXiv:2010.13359*, 2020.

[16] Y. Chen, G. Lan, and Y. Ouyang. Optimal primal-dual methods for a class of saddle point problems. *SIAM Journal on Optimization*, 24(4):1779–1814, Jan. 2014.

[17] Y. Chen, G. Lan, and Y. Ouyang. Accelerated schemes for a class of variational inequalities. *Mathematical Programming*, 165(1):113–149, June 2017.

[18] Z. Chen, Z. Yuan, J. Yi, B. Zhou, E. Chen, and T. Yang. Universal stagewise learning for non-convex problems with convergence on averaged solutions. In *International Conference on Learning Representations*, 2019.

[19] C. Daskalakis, A. Ilyas, V. Syrgkanis, and H. Zeng. Training GANs with optimism. In *International Conference on Learning Representations*, 2018.

[20] E. Delage and Y. Ye. Distributionally robust optimization under moment uncertainty with application to data-driven problems. *Operations research*, 58(3):595–612, 2010.

[21] J. Deng, W. Dong, R. Socher, L.-J. Li, K. Li, and L. Fei-Fei. Imagenet: A large-scale hierarchical image database. In *2009 IEEE conference on computer vision and pattern recognition*, pages 248–255. Ieee, 2009.

[22] Y. Deng, M. M. Kamani, and M. Mahdavi. Distributionally robust federated averaging. In *Advances in Neural Information Processing Systems*, volume 33, pages 15111–15122. Curran Associates, Inc., 2020.

[23] Y. Deng and M. Mahdavi. Local stochastic gradient descent ascent: Convergence analysis and communication efficiency. In *Proceedings of The 24th International Conference on Artificial Intelligence and Statistics*, volume 130 of *Proceedings of Machine Learning Research*, pages 1387–1395. PMLR, 13–15 Apr 2021.

[24] J. Duchi, E. Hazan, and Y. Singer. Adaptive subgradient methods for online learning and stochastic optimization. *Journal of machine learning research*, 12(7), 2011.

[25] A. Ene and H. L. Nguyen. Adaptive and universal single-gradient algorithms for variational inequalities. *arXiv preprint arXiv:2010.07799*, 2020.

[26] G. Gidel, H. Berard, G. Vignoud, P. Vincent, and S. Lacoste-Julien. A variational inequality perspective on generative adversarial networks. In *International Conference on Learning Representations*, 2019.

[27] G. Gidel, R. A. Hemmat, M. Pezeshki, R. Le Priol, G. Huang, S. Lacoste-Julien, and I. Mitliagkas. Negative momentum for improved game dynamics. In *The 22nd International Conference on Artificial Intelligence and Statistics*, pages 1802–1811. PMLR, 2019.

[28] I. J. Goodfellow, J. Pouget-Abadie, M. Mirza, B. Xu, D. Warde-Farley, S. Ozair, A. C. Courville, and Y. Bengio. Generative adversarial nets. In *NIPS*, 2014.

[29] Z. Guo, M. Liu, Z. Yuan, L. Shen, W. Liu, and T. Yang. Communication-efficient distributed stochastic auc maximization with deep neural networks. In *International Conference on Machine Learning*, pages 3864–3874. PMLR, 2020.

[30] M. Heusel, H. Ramsauer, T. Unterthiner, B. Nessler, and S. Hochreiter. Gans trained by a two time-scale update rule converge to a local nash equilibrium. In *NIPS*, 2017.

[31] C. Hou, K. K. Thekumparampil, G. Fanti, and S. Oh. Efficient algorithms for federated saddle point optimization, 2021.

[32] A. Juditsky, A. Nemirovski, et al. First order methods for nonsmooth convex large-scale optimization, ii: utilizing problems structure. *Optimization for Machine Learning*, 30(9):149–183, 2011.

[33] A. Juditsky, A. Nemirovski, and C. Tauvel. Solving variational inequalities with stochastic mirror-prox algorithm. *Stochastic Systems*, 1(1):17–58, June 2011.

[34] D. P. Kingma and J. Ba. Adam: A method for stochastic optimization. In *International Conference on Learning Representations*, 2017.

[35] G. M. Korpelevich. The extragradient method for finding saddle points and other problems. *Matecon*, 1976.

[36] X. Li, K. Huang, W. Yang, S. Wang, and Z. Zhang. On the convergence of fedavg on non-iid data. In *International Conference on Learning Representations*, 2020.

[37] T. Lin, C. Jin, and M. I. Jordan. Near-optimal algorithms for minimax optimization. In *Conference on Learning Theory*, pages 2738–2779. PMLR, 2020.

[38] T. Lin, S. U. Stich, K. K. Patel, and M. Jaggi. Don't use large mini-batches, use local sgd. In *International Conference on Learning Representations*, 2020.

[39] M. Liu, Y. Mroueh, J. Ross, W. Zhang, X. Cui, P. Das, and T. Yang. Towards better understanding of adaptive gradient algorithms in generative adversarial nets. In *International Conference on Learning Representations*, 2020.

[40] M. Liu, W. Zhang, Y. Mroueh, X. Cui, J. Ross, T. Yang, and P. Das. A decentralized parallel algorithm for training generative adversarial nets. volume 33, 2020.

[41] H. B. McMahan et al. Advances and open problems in federated learning. *Foundations and Trends® in Machine Learning*, 14(1), 2021.

[42] P. Mertikopoulos, B. Lecouat, H. Zenati, C.-S. Foo, V. Chandrasekhar, and G. Piliouras. Optimistic mirror descent in saddle-point problems: Going the extra(-gradient) mile. In *International Conference on Learning Representations*, 2019.

[43] P. Mertikopoulos, C. Papadimitriou, and G. Piliouras. Cycles in adversarial regularized learning. In *Proceedings of the Twenty-Ninth Annual ACM-SIAM Symposium on Discrete Algorithms*, pages 2703–2717. SIAM, 2018.

[44] R. D. C. Monteiro and B. F. Svaiter. Complexity of variants of tseng's modified f-b splitting and korpelevich's methods for hemivariational inequalities with applications to saddle-point and convex optimization problems. *SIAM J. Optimization*, 21:1688–1720, 2011.

[45] A. Nemirovski. Prox-method with rate of convergence o (1/t) for variational inequalities with lipschitz continuous monotone operators and smooth convex-concave saddle point problems. *SIAM Journal on Optimization*, 15(1):229–251, 2004.

[46] A. Nemirovski, A. Juditsky, G. Lan, and A. Shapiro. Robust stochastic

approximation approach to stochastic programming. *SIAM Journal on Optimization*, 19(4):1574–1609, 2009.

[47] J. v. Neumann. Zur theorie der gesellschaftsspiele. *Mathematische annalen*, 100(1):295–320, 1928.

[48] S. J. Reddi, Z. Charles, M. Zaheer, Z. Garrett, K. Rush, J. Konečný, S. Kumar, and H. B. McMahan. Adaptive federated optimization. In *International Conference on Learning Representations*, 2021.

[49] S. J. Reddi, S. Kale, and S. Kumar. On the convergence of adam and beyond. In *International Conference on Learning Representations*, 2018.

[50] A. Rogozin, A. Beznosikov, D. Dvinskikh, D. Kovalev, P. Dvurechensky, and A. Gasnikov. Decentralized distributed optimization for saddle point problems, 2021.

[51] A. Smola and S. Narayanamurthy. An architecture for parallel topic models. *Proceedings of the VLDB Endowment*, 3(1-2):703–710, 2010.

[52] S. U. Stich. Local SGD converges fast and communicates little. In *International Conference on Learning Representations*, 2019.

[53] J. Wang, T. Zhang, S. Liu, P.-Y. Chen, J. Xu, M. Fardad, and B. Li. Towards a unified min-max framework for adversarial exploration and robustness. *arXiv preprint arXiv:1906.03563*, 2019.

[54] C. Xie, O. Koyejo, I. Gupta, and H. Lin. Local adaalter: Communication-efficient stochastic gradient descent with adaptive learning rates. *arXiv preprint arXiv:1911.09030*, 2019.

[55] Y. Yan and Y. Xu. Adaptive primal-dual stochastic gradient method for expectation-constrained convex stochastic programs. *arXiv preprint arXiv:2012.14943*, 2020.

[56] H. Yu, R. Jin, and S. Yang. On the linear speed-up analysis of communication efficient momentum SGD for distributed non-convex optimization. In *Proceedings of the 36th International Conference on Machine Learning*, volume 97 of *Proceedings of Machine Learning Research*, pages 7184–7193. PMLR, 09–15 Jun 2019.

[57] J. Zhang, P. Xiao, R. Sun, and Z. Luo. A single-loop smoothed gradient descent-ascent algorithm for nonconvex-concave min-max problems. In *Advances in Neural Information Processing Systems*, volume 33, pages 7377–7389. Curran Associates, Inc., 2020.

[58] R. Zhao. Accelerated stochastic algorithms for convex-concave saddle-point problems. *arXiv preprint arXiv:1903.01687*, 2021.

[59] F. Zou, L. Shen, Z. Jie, W. Zhang, and W. Liu. A sufficient condition for convergences of adam and rmsprop. In *Proceedings of the IEEE/CVF Conference on computer vision and pattern recognition*, pages 11127–11135, 2019.

Appendix A Related Works

Stochastic minimax algorithms. Stochastic convex-concave minimax problems (1) have been extensively studied in the optimization literature and are usually solved via variants of PDHG or extragradient methods, for example, [9, 58, 45, 46, 33, 32, 16, 7]. [17] and [33] adopted mirror-prox-type methods to tackle the stochastic convex-concave minimax problem with $O(1/\sqrt{T})$ convergence rate. [58] proposed an accelerated stochastic PDHG-type algorithm with Bergman divergence to solve the stochastic convex-concave minimax problem with a similar $O(1/\sqrt{T})$ convergence rate dominated by the stochastic variance term. However, while all these algorithms [17, 33, 58] have achieved the optimal rate according to the low and upper bound for the stochastic convex-concave minimax problem [7], their performance is highly influenced by the choice of the learning rate, which is either using sufficiently small constants or diminishing learning rates.

Adaptive minimax algorithms. Adaptive learning rate in stochastic optimization is first developed for minimization problems [24]. Its variants [34, 49, 59, 12, 11] are widely used to train deep learning models. The key feature of the adaptive learning rate is that it can automatically adjust the learning rate during the training process and achieve faster convergence. Recently, the adaptive learning rate has also been developed for minimax algorithms to accelerate the training process, since the learning rate in stochastic minimax algorithm is hard to tune based on the minimax loss, as compared to minimization problems. Several recent papers have tried to analyze the convergence rate of adaptive extragradient in the convex-concave minimax settings. The universal mirror-prox method [6] proposed a new adaptive learning rate technique that adapts to problem parameters, such as the unknown Lipschitz parameter, and achieves optimal convergence rates in stochastic setting. [5] extended the universal mirror-prox [6] by replacing the norm dependence in the learning rate with a general Bregman divergence dependence. [25] proposed an adaptive stochastic single-call extragradient algorithm for variational inequality problems. [1] proposed a similar adaptive mirror-prox algorithm, but their method handles an unbounded domain by introducing the notion of local norms in the deterministic setting. In addition to the adaptive extragradient methods mentioned above for the general stochastic minimax problem, [55] proposed an adaptive primal-dual method for expectation-constrained convex stochastic programs, which can be formulated as a minimax optimization with the coupled term being a linear function with dual variable. Training of a GAN model [28] corresponds to solving a specific non-convex non-concave minimax problem. Several works have heuristically adopted a stochastic adaptive extragradient for training GANs [26, 42, 7]. Recently, [39] studied the convergence behavior of an adaptive optimistic stochastic gradient algorithm for a class of non-convex non-concave minimax problems under the MVI condition to train GANs.

Distributed minimax algorithms. As datasets and deep learning architectures become larger and larger distributed minimax algorithms are needed for GANs and adversarial training. [7] established upper and lower bounds for iteration complexity for strongly-convex-strongly-concave and convex-concave minimax problems in both a centralized and decentralized setting. However, the convergence rate for their Extra Step Local SGD is established only in a strongly-convex-strongly-concave setting with a linear speed-up property with respect to the number of works; while for their proposed local Adam no convergence results are provided. [23] provided convergence guarantees for a primal-dual local stochastic gradient algorithm in the strongly-convex-strongly-concave-setting and several non-convex settings with PL-inequality-type conditions. [15] and [40] studied the convergence of a distributed optimistic stochastic gradient algorithm for non-convex non-concave minimax problems under the pseudomonotonicity condition and MVI condition, respectively. However, their convergence rates hold only for a sufficiently large minibatch size or a sufficiently large number of workers. In addition, there also exist several decentralized or federated algorithms for stochastic strongly-convex-strongly-concave minimax problems [31, 50]. In this work, we mainly focus on the centralized setting for the stochastic convex-concave minimax problems.

Appendix B Appendix to Main Text

B.1 Extension to Unbounded Stochastic Gradient Oracle

Let $\{Z_i\}_{i=1}^n$ be a sequence of i.i.d. standard normals. We have the following well-known results (see Appendix A of [10]):

$$\mathbb{P}\big(\max_i Z_i > \mathbb{E}[\max_i Z_i] + t\big) \leq \exp(-t^2/2) \text{ for all } t > 0,$$
$$\mathbb{E}[\max_i |Z_i|] \leq \sqrt{2\log(2n)}.$$

With this, we have $\mathbb{P}(\max_i |Z_i| \geq \sqrt{2\log(2n)} + t) \leq 2\exp(-t^2/2)$. We apply this result to the sequence $\big\{\|G(z_t^m) - \tilde{G}(z_t^m)\|_*/\|G\|_\infty, \|G(\tilde{z}_{t-1}^{m,*}) - \tilde{G}(\tilde{z}_{t-1}^{m,*})\|_*/\|G\|_\infty\big\}_{m,t}$, which is a sequence of $2MT$ i.i.d. standard normals by the homogeneity of the oracle.

Appendix C Proof of Theorems

Lemma 3 For all $m \in [M]$, consider the sequence $\{\eta_t^m, \tilde{z}_{t-1}^{m,*}, z_t^m, \tilde{z}_t^m\}_{t=1}^T$ defined in Algorithm 1. It holds

$$\|\tilde{z}_{t-1}^{m,*} - z_t^m\|/\eta_t^m \leq G, \quad \|\tilde{z}_t^m - z_t^m\|/\eta_t^m \leq G.$$

Proof of Lemma 3 Let $I : \mathcal{Z} \to \mathcal{Z}^*$ be the identity map which maps an element $z \in \mathcal{Z}$ to the corresponding element in the dual space $\mathcal{Z}^*$ (we are considering Euclidean case). The first-order optimality condition of the update rule $z_t^m = \Pi_{\mathcal{Z}}[\tilde{z}_{t-1}^{m,*} - \eta_t^m M_t^m]$ is

$$\langle \eta_t^m M_t^m + I(z_t^m - \tilde{z}_{t-1}^{m,*}), z - z_t^m \rangle \geq 0, \forall z \in \mathcal{Z}.$$

Set $z = \tilde{z}_{t-1}^{m,*}$, apply the Cauchy-Schwartz inequality and we obtain

$$\begin{aligned}\eta_t^m \|M_t^m\|_* \cdot \|\tilde{z}_{t-1}^{m,*} - z_t^m\| &\geq \langle \eta_t^m M_t^m, \tilde{z}_{t-1}^{m,*} - z_t^m \rangle \\ &\geq \langle I(\tilde{z}_{t-1}^{m,*} - z_t^m), \tilde{z}_{t-1}^{m,*} - z_t^m \rangle = \|\tilde{z}_{t-1}^{m,*} - z_t^m\|^2.\end{aligned}$$

The second inequality holds due to similar reasoning. We conclude the proof of Lemma 3. □

Lemma 4 (One-step analysis) For all $m \in [M]$, consider the sequence $\{\eta_t^m, \tilde{z}_{t-1}^{m,*}, M_t^m = \tilde{G}(\tilde{z}_{t-1}^{m,*}), z_t^m, g_t^m = \tilde{G}(\tilde{z}_t^m), \tilde{z}_t^m\}_{t=1}^T$ defined in Algorithm 1. It holds for all $z \in \mathcal{Z}$,

$$\begin{aligned}\langle z_t^m - z, g_t^m \rangle \leq \frac{1}{\eta_t^m}\left(\tfrac{1}{2}\|z - \tilde{z}_{t-1}^{m,*}\|^2 - \tfrac{1}{2}\|z - \tilde{z}_t^m\|^2\right) - \frac{1}{\eta_t^m}\left(\tfrac{1}{2}\|z_t^m - \tilde{z}_{t-1}^{m,*}\|^2 + \tfrac{1}{2}\|z_t^m - \tilde{z}_t^m\|^2\right) \\ + \|g_t^m - M_t^m\|_* \cdot \|z_t^m - \tilde{z}_t^m\|.\end{aligned}$$

Proof of Lemma 4 For any $c, g \in \mathcal{Z}$, consider the update of the form $a^* = \Pi_{\mathcal{Z}}[c - g] = \operatorname{argmin}_{z \in \mathcal{Z}} \langle g, z \rangle + \frac{1}{2}\|z - c\|^2$. It holds for all $b \in \mathcal{Z}$,

$$\langle g, a^* - b \rangle \leq \tfrac{1}{2}\|b - c\|^2 - \tfrac{1}{2}\|b - a^*\|^2 - \tfrac{1}{2}\|a^* - c\|^2.$$

By the update rule of z_t^m and $\tilde{z}_t^m$, we have (taking $a^* \leftrightarrow z_t^m$, $b \leftrightarrow \tilde{z}_t^m$, $g \leftrightarrow \eta_t^m M_t^m$, $c \leftrightarrow \tilde{z}_{t-1}^{m,*}$)

$$\langle \eta_t^m M_t^m, z_t^m - \tilde{z}_t^m \rangle \leq \tfrac{1}{2}\|\tilde{z}_t^m - \tilde{z}_{t-1}^{m,*}\|^2 - \tfrac{1}{2}\|\tilde{z}_t^m - z_t^m\|^2 - \tfrac{1}{2}\|z_t^m - \tilde{z}_{t-1}^{m,*}\|^2, \quad \text{(C1)}$$

and for all $z \in \mathcal{Z}$ (taking $a^* \leftrightarrow \tilde{z}_t^m$, $b \leftrightarrow z$, $g \leftrightarrow \eta_t^m g_t^m$, $c \leftrightarrow \tilde{z}_{t-1}^{m,*}$)

$$\langle \eta_t^m g_t^m, \tilde{z}_t^m - z \rangle \leq \tfrac{1}{2}\|z - \tilde{z}_{t-1}^{m,*}\|^2 - \tfrac{1}{2}\|z - \tilde{z}_t^m\|^2 - \tfrac{1}{2}\|\tilde{z}_t^m - \tilde{z}_{t-1}^{m,*}\|^2. \quad \text{(C2)}$$

Finally we apply the Cauchy-Schwarz inequality and plug in Eqs. (C1) and (C2).

$$\begin{aligned}\langle g_t^m, z_t^m - z \rangle &= \langle g_t^m, z_t^m - \tilde{z}_t^m \rangle + \langle g_t^m, \tilde{z}_t^m - z \rangle \\ &= \langle g_t^m - M_t^m, z_t^m - \tilde{z}_t^m \rangle + \langle g_t^m, \tilde{z}_t^m - z \rangle + \langle M_t^m, z_t^m - \tilde{z}_t^m \rangle \\ &\leq \|g_t^m - M_t^m\|_* \cdot \|z_t^m - \tilde{z}_t^m\| + \langle g_t^m, \tilde{z}_t^m - z \rangle + \langle M_t^m, z_t^m - \tilde{z}_t^m \rangle \\ &\leq \|g_t^m - M_t^m\|_* \cdot \|z_t^m - \tilde{z}_t^m\| \\ &\quad + \frac{1}{\eta_t^m}\left(\tfrac{1}{2}\|\tilde{z}_t^m - \tilde{z}_{t-1}^{m,*}\|^2 - \tfrac{1}{2}\|\tilde{z}_t^m - z_t^m\|^2 - \tfrac{1}{2}\|z_t^m - \tilde{z}_{t-1}^{m,*}\|^2\right) \\ &\quad + \frac{1}{\eta_t^m}\left(\tfrac{1}{2}\|z - \tilde{z}_{t-1}^{m,*}\|^2 - \tfrac{1}{2}\|z - \tilde{z}_t^m\|^2 - \tfrac{1}{2}\|\tilde{z}_t^m - \tilde{z}_{t-1}^{m,*}\|^2\right) \\ &= \frac{1}{\eta_t^m}\left(\tfrac{1}{2}\|z - \tilde{z}_{t-1}^{m,*}\|^2 - \tfrac{1}{2}\|z - \tilde{z}_t^m\|^2\right) - \frac{1}{\eta_t^m}\left(\tfrac{1}{2}\|z_t^m - \tilde{z}_{t-1}^{m,*}\|^2 + \tfrac{1}{2}\|z_t^m - \tilde{z}_t^m\|^2\right) \\ &\quad + \|g_t^m - M_t^m\|_* \cdot \|z_t^m - \tilde{z}_t^m\|.\end{aligned}$$

This finishes the proof of Lemma 4. □

C.1 Proof of Theorem 1

Proof of Theorem 1, Non-smooth Case The proof strategy follows closely that of Bach and Levy [6]. **Step 1.** We apply the Lemma 4 and sum over all $m \in [M]$ and $t \in [T]$. Define

$$\xi_t^m := G(z_t^m) - g_t^m = G(z_t^m) - \tilde{G}(z_t^m).$$

For all $z \in \mathcal{Z}$,

$$\sum_{t=1}^{T}\sum_{m=1}^{M} \langle z_t^m - z, G(z_t^m)\rangle = \sum_{t=1}^{T}\sum_{m=1}^{M} \langle z_t^m - z, \xi_t^m\rangle + \sum_{t=1}^{T}\sum_{m=1}^{M} \langle z_t^m - z, g_t^m\rangle \tag{C3}$$

$$\leq \underbrace{\sum_{t=1}^{T}\sum_{m=1}^{M} \langle z_t^m - z, \xi_t^m\rangle}_{I(z)} \tag{C4}$$

$$+ \underbrace{\sum_{t=1}^{T}\sum_{m=1}^{M} \frac{1}{\eta_t^m}\left(\tfrac{1}{2}\|z - \tilde{z}_{t-1}^{m,*}\|^2 - \tfrac{1}{2}\|z - \tilde{z}_t^m\|^2\right)}_{II(z)} \tag{C5}$$

$$\underbrace{-\sum_{t=1}^{T}\sum_{m=1}^{M} \frac{1}{\eta_t^m}\left(\tfrac{1}{2}\|z_t^m - \tilde{z}_{t-1}^{m,*}\|^2 + \tfrac{1}{2}\|z_t^m - \tilde{z}_t^m\|^2\right)}_{III} \tag{C6}$$

$$+ \underbrace{\sum_{t=1}^{T}\sum_{m=1}^{M} \|g_t^m - M_t^m\|_* \cdot \|z_t^m - \tilde{z}_t^m\|}_{IV}. \tag{C7}$$

Now we use Lemma 8 and obtain

$$TM \cdot \mathbb{E}[\text{DualGap}(\bar{z})] \leq \mathbb{E}[\sup_{z\in\mathcal{Z}}\{I(z) + II(z) + III + IV\}] \tag{C8}$$

$$\leq \mathbb{E}[\sup_{z\in\mathcal{Z}} I(z)] + \mathbb{E}[\sup_{z\in\mathcal{Z}} II(z)] + \mathbb{E}[III] + \mathbb{E}[IV] \tag{C9}$$

Next we upper bound each term in turns. Steps 2–5 rely heavily on the learning rate scheme. Define

$$(Z_t^m)^2 := \frac{\|z_t^m - \tilde{z}_{t-1}^{m,*}\|^2 + \|z_t^m - \tilde{z}_t^m\|^2}{5(\eta_t^m)^2}$$

for all $t \in [T]$ and $m \in [M]$. By Lemma 3 we know $Z_t^m \leq G$ almost surely. This is due to

$$\|z_t^m - \tilde{z}_{t-1}^{m,*}\|^2 + \|z_t^m - \tilde{z}_t^m\|^2 \leq \|z_t^m - \tilde{z}_{t-1}^{m,*}\|^2 + 2\|z_t^m - \tilde{z}_{t-1}^{m,*}\|^2 + 2\|\tilde{z}_{t-1}^{m,*} - \tilde{z}_t^m\|^2 \leq 5G^2(\eta_t^m)^2.$$

Moreover, for the nonsmooth case ($\alpha = 1$), η_t^m can be expressed by

$$\eta_t^m = \frac{D}{\sqrt{G_0^2 + \sum_{\tau=1}^{t-1}(Z_\tau^m)^2}}. \tag{C10}$$

Step 2. Show $\mathbb{E}[\sup_{z\in\mathcal{Z}} I(z)] = O(\sigma D\sqrt{MT})$. For all $z \in \mathcal{Z}$,

$$I(z) = \sum_{t=1}^{T}\sum_{m=1}^{M} \langle z_t^m - \tilde{z}_0^m, \xi_t^m\rangle + \sum_{t=1}^{T}\sum_{m=1}^{M} \langle \tilde{z}_0^m - z, \xi_t^m\rangle.$$

The first term is a martingale difference sequence (MDS) and is zero in expectation. For the second term, we use the Cauchy–Schwarz inequality. For all $z \in \mathcal{Z}$,

$$\begin{aligned}\mathbb{E}\Big[\sup_z \sum_{t=1}^{T}\sum_{m=1}^{M}\langle \tilde{z}_0^m - z, \xi_t^m\rangle\Big] &= \mathbb{E}\Big[\sup_z \Big\langle \tilde{z}_0 - z, \sum_{t=1}^{T}\sum_{m=1}^{M}\xi_t^m\Big\rangle\Big] \\ &\le \mathbb{E}\Big[\sup_z \|\tilde{z}_0 - z\| \cdot \Big\|\sum_{t=1}^{T}\sum_{m=1}^{M}\xi_t^m\Big\|_*\Big] \\ &\le D \cdot \sqrt{\mathbb{E}\Big[\Big\|\sum_{t=1}^{T}\sum_{m=1}^{M}\xi_t^m\Big\|_*^2\Big]} \le \sigma D\sqrt{MT}.\end{aligned}$$

In the last equality, we use the fact that $\{\xi_t^m\}$ is an MDS. This establishes $\mathbb{E}[\sup_z I(z)] \le \sigma D\sqrt{MT}$.

Step 3. Show $\mathbb{E}[\sup_{z\in\mathcal{Z}} II(z)] = O(DG \cdot M\sqrt{T})$. For all $z \in \mathcal{Z}$,

$$\begin{aligned}II(z) &= \sum_{t=1}^{T}\sum_{m=1}^{M}\frac{1}{\eta_t^m}\big(\tfrac{1}{2}\|z - \tilde{z}_{t-1}^{m,*}\|^2 - \tfrac{1}{2}\|z - \tilde{z}_t^m\|^2\big) \\ &= \sum_{m=1}^{M}\sum_{t\notin S+1}\frac{1}{\eta_t^m}\big(\tfrac{1}{2}\|z - \tilde{z}_{t-1}^{m,*}\|^2 - \tfrac{1}{2}\|z - \tilde{z}_t^m\|^2\big) + \sum_{m=1}^{M}\sum_{t\in S+1}\frac{1}{\eta_t^m}\big(\tfrac{1}{2}\|z - \tilde{z}_{t-1}^{m,*}\|^2 - \tfrac{1}{2}\|z - \tilde{z}_t^m\|^2\big) \\ &= \sum_{m=1}^{M}\sum_{t\notin S+1}\frac{1}{\eta_t^m}\big(\tfrac{1}{2}\|z - \tilde{z}_{t-1}^{m}\|^2 - \tfrac{1}{2}\|z - \tilde{z}_t^m\|^2\big) + \sum_{m=1}^{M}\sum_{t\in S+1}\frac{1}{\eta_t^m}\big(\tfrac{1}{2}\|z - \tilde{z}_{t-1}^{\circ}\|^2 - \tfrac{1}{2}\|z - \tilde{z}_t^m\|^2\big) \\ &= \underbrace{\sum_{m=1}^{M}\sum_{t=1}^{T}\frac{1}{\eta_t^m}\big(\tfrac{1}{2}\|z - \tilde{z}_{t-1}^{m}\|^2 - \tfrac{1}{2}\|z - \tilde{z}_t^m\|^2\big)}_{A} + \underbrace{\sum_{m=1}^{M}\sum_{t\in S+1}\frac{1}{\eta_t^m}\big(\tfrac{1}{2}\|z - \tilde{z}_{t-1}^{\circ}\|^2 - \tfrac{1}{2}\|z - \tilde{z}_{t-1}^{m}\|^2\big)}_{B}\end{aligned}$$

where we used the definition of $\tilde{z}_{t-1}^{m,*}$ for two cases $t \in S+1$ and $t \notin S+1$ (Line 8 and 10 in algorithm).

We upper bound A and show $B \le 0$.

Recall for $t \in S+1$, we have $\tilde{z}_{t-1}^{m,*} = \tilde{z}_{t-1}^{\circ} = \sum_{m=1}^{M} w_m \cdot \tilde{z}_{t-1}^m$, and for $t \notin S+1$, we have $\tilde{z}_{t-1}^{m,*} = \tilde{z}_{t-1}^m$. For the first term A we use $\frac{1}{2}\|z - \tilde{z}_t^m\|^2 \le D^2$ and then telescope.

$$\begin{aligned}A &= \sum_{m=1}^{M}\Big[\frac{1}{\eta_1^m}\Big(\tfrac{1}{2}\|\tilde{z}_0^m - z\|^2\Big) - \frac{1}{\eta_T^m}\Big(\tfrac{1}{2}\|\tilde{z}_T^m - z\|^2\Big) + \sum_{t=2}^{T}\Big(\frac{1}{\eta_t^m} - \frac{1}{\eta_{t-1}^m}\Big)\Big(\tfrac{1}{2}\|\tilde{z}_{t-1}^m - z\|^2\Big)\Big] \\ &\le \sum_{m=1}^{M}\Big[\frac{D^2}{\eta_1^m} + \sum_{t=2}^{T}\Big(\frac{1}{\eta_t^m} - \frac{1}{\eta_{t-1}^m}\Big)D^2\Big] \\ &\le \sum_{m=1}^{M}\Big[\frac{D^2}{\eta_1^m} + \frac{D^2}{\eta_T^m}\Big]\end{aligned}$$

For each m, we have $D^2/\eta_1^m = DG_0$. For D^2/η_T^m we use the learning rate scheme. Recall the definition of Z_t^m. Then

$$\frac{D^2}{\eta_T^m} = D\sqrt{G_0^2 + \sum_{t=1}^{T-1}(Z_t^m)^2} \le D\sqrt{G_0 + G^2T} \le DG_0 + DG\sqrt{T}.$$

This implies $A \le M(2DG_0 + DG\sqrt{T}) = O(DG \cdot M\sqrt{T})$.

For the term B, we use the definition of $\tilde{z}_{t-1}^{\circ}$ and the weights $\{w_m\}$ to show $B \le 0$. For each t, since $\tilde{z}_{t-1}^{\circ}$ the same for all workers,

$$\begin{aligned}
\sum_{m=1}^{M} \frac{1}{\eta_t^m}\Big(\tfrac{1}{2}\|z - \tilde{z}_{t-1}^{\circ}\|^2\Big) &= \Big(\sum_{m=1}^{M} \frac{1}{\eta_t^m}\Big)\Big(\tfrac{1}{2}\|z - \tilde{z}_{t-1}^{\circ}\|^2\Big) \\
&= \Big(\sum_{m=1}^{M} \frac{1}{\eta_t^m}\Big)\Big(\tfrac{1}{2}\big\|\textstyle\sum_{m=1}^{M} {w_m}^{1/2} \cdot {w_m}^{1/2}(z - \tilde{z}_{t-1}^{m})\big\|^2\Big) \\
&\le \Big(\sum_{m=1}^{M} \frac{1}{\eta_t^m}\Big)\Big(\sum_{m=1}^{M} w_m\Big)\Big(\sum_{m=1}^{M} w_m \cdot \tfrac{1}{2}\|z - \tilde{z}_{t-1}^{m}\|^2\Big) \\
&= \sum_{m=1}^{M} \frac{1}{\eta_t^m}\Big(\tfrac{1}{2}\|z - \tilde{z}_{t-1}^{m}\|^2\Big).
\end{aligned}$$

In the last equality we use $\sum_{m=1}^{M} w_m = 1$ and $(\sum_{m=1}^{M} 1/\eta_t^m) w_{m'} = 1/\eta_t^{m'}$ for all $m' \in [M]$. This implies $B \le 0$. This establishes $\mathbb{E}[\sup_z II(z)] \le \mathbb{E}[\sup_z A] = O(DG \cdot M\sqrt{T})$.

Step 4. Show $\mathbb{E}[III] \le 0$. This is obviously true.

Step 5. Show $\mathbb{E}[IV] = \tilde{O}(\gamma DG \cdot M\sqrt{T})$. Define $\gamma = G/G_0$. By 2 we have $\|g_t^m - M_t^m\|_* \le 2G$. It holds almost surely that

$$\begin{aligned}
IV &\le 2G \sum_{m=1}^{M}\sum_{t=1}^{T} \|z_t^m - \tilde{z}_t^m\| \\
&\le 2G\sqrt{T} \cdot \sum_{m=1}^{M} \sqrt{\sum_{t=1}^{T} \|z_t^m - \tilde{z}_t^m\|^2} \\
&\le 2G\sqrt{T} \cdot \sum_{m=1}^{M} \sqrt{\sum_{t=1}^{T} (\eta_t^m Z_t^m)^2} \\
&= 2G\sqrt{T} \cdot D \cdot \sum_{m=1}^{M} \sqrt{\sum_{t=1}^{T} \frac{(Z_t^m)^2}{G_0^2 + \sum_{\tau=1}^{t-1} (Z_\tau^m)^2}} \\
&\le 2GD\sqrt{T} \cdot \sum_{m=1}^{M} \sqrt{2 + 4\gamma^2 + 2\log\Big(\frac{G_0^2 + \sum_{t=1}^{T-1} (Z_t^m)^2}{G_0^2}\Big)} \qquad \text{(Lemma 6)} \\
&\le 2GD\sqrt{T} \cdot \sum_{m=1}^{M} \sqrt{2 + 4\gamma^2 + 2\log\Big(\frac{G_0^2 + G^2 T}{G_0^2}\Big)} \\
&\le 2GD\sqrt{T} \cdot \sum_{m=1}^{M} \sqrt{2 + 4\gamma^2 + 2\log(1 + \gamma^2 T)}
\end{aligned}$$

$$= \tilde{O}(\gamma GD \cdot M\sqrt{T})$$

Finally, we plug in the upper bounds for I–IV and continue Eq (C9).

$$TM \cdot \mathbb{E}[\text{DualGap}(\bar{z})] = \tilde{O}(\gamma DG \cdot M\sqrt{T} + \sigma D\sqrt{MT}).$$

This finishes the proof of Theorem 1 □

C.2 Proof of Theorem 2

Proof of Theorem 2, Smooth Case The proof strategy follows closely that of Bach and Levy [6]. Using the notation for Step 1 in the proof for the nonsmooth case, we have the bound

$$TM\mathbb{E}[\text{DualGap}(\bar{z})] \leq \mathbb{E}[\sup_z\{I(z) + II(z) + III + IV\}],$$

where I–IV are defined in Eqs. (C4)–(C7). We deal with these terms in a different manner.

For the term $I(z)$ in Eq. (C4), following Step 2 we have $\mathbb{E}[\sup_z I(z)] = O(\gamma\sigma D\sqrt{MT})$.

Next, we define a stopping time. For each $m \in [M]$, let

$$\tau_m^* := \max\left\{t \in [T] : \frac{1}{\eta_t^m} \leq 1/(2L)\right\}. \tag{C11}$$

Recall our learning rate scheme for the smooth case

$$\eta_1^m = \frac{D\alpha}{G_0}, \quad \eta_t^m = \frac{D\alpha}{\sqrt{G_0^2 + \sum_{\tau=1}^{t-1}(Z_\tau^m)^2}}.$$

For the term $II(z)$ in Eq. (C5), we follow Step 3 and obtain for all $z \in \mathcal{Z}$,

$$II(z) \leq \sum_{m=1}^{M}\left(\frac{D^2}{\eta_1^m} + \frac{D^2}{\eta_T^m}\right).$$

By the definition of η_1^m, we have $\sum_{m=1}^M D^2/\eta_1^m \leq DMG_0/\alpha$. For the second term, for fixed $m \in [M]$,

$$\sum_{m=1}^{M} D^2/\eta_T^m = \sum_{m=1}^{M}\frac{D}{\alpha}\sqrt{G_0^2 + \sum_{t=1}^{T-1}(Z_t^m)^2} \tag{C12}$$

$$\leq \sum_{m=1}^{M}\frac{D}{\alpha}\left(G_0 + \sum_{t=1}^{T}\frac{(Z_t^m)^2}{\sqrt{G_0^2 + \sum_{\tau=1}^{t-1}(Z_\tau^m)^2}}\right) \quad \text{(Lemma 7)}$$

$$= \frac{MDG_0}{\alpha} + \underbrace{\sum_{m=1}^{M}\sum_{t=1}^{T}\frac{1}{\alpha^2}\eta_t^m(Z_t^m)^2}_{:=\mathcal{A}} \tag{C13}$$

So we have $\mathbb{E}[\sup_z II(z)] \leq 2\gamma MDG/\alpha + \mathbb{E}[\mathcal{A}]$.

For the term III in Eq. (C6), we also split it into two parts by τ_m^*.

$$III := -\sum_{t=1}^{T}\sum_{m=1}^{M}\frac{1}{\eta_t^m}\left(\tfrac{1}{2}\|z_t^m - \tilde{z}_{t-1}^{m,*}\|^2 + \tfrac{1}{2}\|z_t^m - \tilde{z}_t^m\|^2\right) \tag{C14}$$

$$= -\sum_{t=1}^{T}\sum_{m=1}^{M}\frac{5}{2}\eta_t^m(Z_t^m)^2 \tag{C15}$$

$$= \underbrace{-\sum_{m=1}^{M}\sum_{t=1}^{\tau_m^*}\frac{5}{2}\eta_t^m(Z_t^m)^2}_{\geq 0} \underbrace{-\sum_{m=1}^{M}\sum_{t=\tau_m^*+1}^{T}\frac{5}{2}\eta_t^m(Z_t^m)^2}_{:=\mathcal{B}_{\text{tail}}} \tag{C16}$$

For the term IV in defined in Eq. (C7), we first introduce a margtingale difference sequence. For all $t \in [T], m \in [M]$, let

$$\zeta_t^m := \big(g_t^m - G(z_t^m)\big) + \big(M_t^m - G(\tilde{z}_{t-1}^{m,*})\big). \tag{C17}$$

By the triangular inequality, we have

$$IV := \sum_{t=1}^{T}\sum_{m=1}^{M}\|g_t^m - M_t^m\|_* \cdot \|z_t^m - \tilde{z}_t^m\| \tag{C18}$$

$$\leq \underbrace{\sum_{t=1}^{T}\sum_{m=1}^{M}\|\zeta_t^m\|_* \cdot \|z_t^m - \tilde{z}_t^m\|}_{:=V} + \sum_{t=1}^{T}\sum_{m=1}^{M}\|G(z_t^m) - G(\tilde{z}_{t-1}^{m,*})\|_* \cdot \|z_t^m - \tilde{z}_t^m\| \tag{C19}$$

$$\leq V + \sum_{t=1}^{T}\sum_{m=1}^{M}\Big(\frac{L}{2}\|z_t^m - \tilde{z}_{t-1}^{m,*}\|^2 + \frac{L}{2}\|z_t^m - \tilde{z}_t^m\|^2\Big) \tag{C20}$$

$$= V + \sum_{t=1}^{T}\sum_{m=1}^{M}\frac{5L}{2}(\eta_t^m)^2(Z_t^m)^2 \tag{C21}$$

$$= V + \underbrace{\sum_{m=1}^{M}\sum_{t=1}^{\tau_m^*}\frac{5L}{2}(\eta_t^m)^2(Z_t^m)^2}_{:=\mathcal{C}_{\text{head}}} + \underbrace{\sum_{m=1}^{M}\sum_{t=\tau_m^*+1}^{T}\frac{5L}{2}(\eta_t^m)^2(Z_t^m)^2}_{:=\mathcal{C}_{\text{tail}}} \tag{C22}$$

Eq. (C20) holds due to smoothness, i.e., for all $z, z' \in \mathcal{Z}$, $\|G(z) - G(z')\|_* \leq L\|z - z'\|$. Using smoothness, we can verify Eq. (C20) as follows.

$$\begin{aligned}
&\|G(z_t^m) - G(\tilde{z}_{t-1}^{m,*})\|_* \cdot \|z_t^m - \tilde{z}_t^m\| \\
&\leq \frac{1}{2L}\|G(z_t^m) - G(\tilde{z}_{t-1}^{m,*})\|_*^2 + \frac{L}{2}\|z_t^m - \tilde{z}_t^m\|^2 \\
&\leq \frac{L}{2}\|z_t^m - \tilde{z}_{t-1}^{m,*}\|^2 + \frac{L}{2}\|z_t^m - \tilde{z}_t^m\|^2.
\end{aligned}$$

To summarize, we have shown

$$TM \cdot \mathbb{E}[\text{DualGap}(\bar{z})] \leq \mathbb{E}[\sup_z\{I(z) + II(z) + III + IV\}] \tag{C23}$$

$$\leq O\Big(\gamma\sigma D\sqrt{MT}\Big) + 2\gamma MDG/\alpha \tag{C24}$$

$$+ \mathbb{E}[\mathcal{A} + \mathcal{C}_{\text{head}} + (-\mathcal{B}_{\text{tail}} + \mathcal{C}_{\text{tail}}) + V]. \tag{C25}$$

Step a. Show $\mathbb{E}[\mathcal{A}] \leq 8\gamma GDM/\alpha + 3DM\mathcal{V}_1(T)/\alpha$. Recall its definition in Eq. (C13).

$$\mathcal{A} := \sum_{m=1}^{M}\sum_{t=1}^{T}\frac{1}{\alpha^2}\eta_t^m(Z_t^m)^2$$

$$= \frac{D}{\alpha}\sum_{m=1}^{M}\sum_{t=1}^{T}\frac{(Z_t^m)^2}{\sqrt{G_0^2+\sum_{\tau=1}^{t-1}(Z_\tau^m)^2}}$$
$$\le \frac{D}{\alpha}\sum_{m=1}^{M}\left(5\gamma G+3\sqrt{G_0^2+\sum_{t=1}^{T-1}(Z_t^m)^2}\right) \quad \text{(Lemma 7)}$$
$$\le \frac{D}{\alpha}\sum_{m=1}^{M}\left(8\gamma G+3\sqrt{\sum_{t=1}^{T-1}(Z_t^m)^2}\right)$$

Note by Lemma 3 we know $(Z_t^m)^2 \le (\|g_t^m\|_*^2+\|M_t^m\|_*^2)/5 \le \|g_t^m\|_*^2+\|M_t^m\|_*^2$. Recall the definition of $\mathcal{V}_m(T)$ in Eq. (6). By the symmetry of the algorithm over all workers, we know $\mathcal{V}_1(T)=\mathcal{V}_m(T)$ for all $m\in[M]$. Then

$$\mathbb{E}[\mathcal{A}] \le 8\gamma DMG/\alpha+\frac{3D}{\alpha}\sum_{m=1}^{M}\mathbb{E}\left[\sqrt{\sum_{t=1}^{T-1}(Z_t^m)^2}\right]$$
$$\le 8\gamma DMG/\alpha+\frac{3D}{\alpha}\sum_{m=1}^{M}\mathbb{E}\left[\sqrt{\sum_{t=1}^{T-1}\|g_t^m\|_*^2+\|M_t^m\|_*^2}\right]$$
$$= 8\gamma DMG/\alpha+\frac{3D}{\alpha}\sum_{m=1}^{M}\mathcal{V}_m(T) = 8\gamma DMG/\alpha+3DM\mathcal{V}_1(T)/\alpha.$$

By our choice of α we have $\mathbb{E}[\mathcal{A}]=O(\gamma DM^{3/2}G+DM^{3/2}\mathcal{V}_1(T))$.

Step b. Show $\mathbb{E}[\mathcal{C}_{\text{head}}]=O(1)$. Recall its definition in Eq. (C22).

$$\mathcal{C}_{\text{head}} := \sum_{m=1}^{M}\sum_{t=1}^{\tau_m^*}\frac{5L}{2}(\eta_t^m)^2(Z_t^m)^2 \quad \text{(C26)}$$
$$= \frac{5\alpha^2D^2L}{2}\sum_{m=1}^{M}\sum_{t=1}^{\tau_m^*}\frac{(Z_t^m)^2}{G_0^2+\sum_{\tau=1}^{t-1}(Z_\tau^m)^2} \quad \text{(C27)}$$
$$\le \frac{5\alpha^2D^2L}{2}\sum_{m=1}^{M}\left(6\gamma^2+2\log\left(\frac{G_0^2+\sum_{t=1}^{\tau_m^*-1}(Z_\tau^m)^2}{G_0^2}\right)\right) \quad \text{(Lemma 6)}$$
$$= \frac{5\alpha^2D^2L}{2}\sum_{m=1}^{M}\left(6\gamma^2+2\log\left(\frac{\alpha^2D^2}{G_0^2(\eta_{\tau_m^*}^m)^2}\right)\right) \quad \text{(C28)}$$
$$\le \frac{5\alpha^2D^2LM}{2}\left(6\gamma^2+4\log\left(\frac{\alpha D}{2G_0L}\right)\right) \quad \text{(C29)}$$

The last inequality is due to the definition of τ_m^*. By our choice of α we have $\mathbb{E}[\mathcal{C}_{\text{head}}]=\tilde{O}(\gamma^2LD^2)$.

Step c. Show $\mathcal{C}_{\text{tail}}-\mathcal{B}_{\text{tail}}\le 0$. Recall $\mathcal{B}_{\text{tail}}$ is defined in Eq. (C16). By definition,

$$\mathcal{C}_{\text{tail}}-\mathcal{B}_{\text{tail}} = \sum_{m=1}^{M}\sum_{t=\tau_m^*+1}^{T}\left(\frac{5L}{2}\eta_t^m-\frac{5}{2}\right)\eta_t^m(Z_t^m)^2.$$

We show $\frac{5L}{2}\eta_t^m-\frac{5}{2}\le 0$ for all $t\in[T], m\in[M]$. Note that for all $t\ge\tau_m^*+1$ we have $\eta_t^m\le 1/(2L)$. And so $\frac{5L}{2}\eta_t^m-\frac{5}{2}\le(5/4)-(5/2)=-5/4$. Summarizing, we have shown $\mathcal{C}_{\text{tail}}-\mathcal{B}_{\text{tail}}\le 0$.

Step d. Show $\mathbb{E}[V] = \tilde{O}(\gamma\sigma D\sqrt{MT})$. Recall its definition in Eq.(C19). Also note $\mathbb{E}[\|\zeta_t^m\|_*^2] \le 4\sigma^2$.

$$\mathbb{E}[V] := \mathbb{E}\left[\sum_{t=1}^{T}\sum_{m=1}^{M}\|\zeta_t^m\|_* \cdot \|z_t^m - \tilde{z}_t^m\|\right] \tag{C30}$$

$$\le \mathbb{E}\left[\sqrt{\sum_{t=1}^{T}\sum_{m=1}^{M}\|\zeta_t^m\|_*^2}\right] \cdot \mathbb{E}\left[\sqrt{\sum_{t=1}^{T}\sum_{m=1}^{M}\|z_t^m - \tilde{z}_t^m\|^2}\right] \tag{C31}$$

$$\le \sqrt{\sum_{t=1}^{T}\sum_{m=1}^{M}\mathbb{E}\big[\|\zeta_t^m\|_*^2\big]} \cdot \mathbb{E}\left[\sqrt{\sum_{t=1}^{T}\sum_{m=1}^{M}\|z_t^m - \tilde{z}_t^m\|^2}\right] \tag{C32}$$

$$\le 2\sigma\sqrt{MT} \cdot \mathbb{E}\left[\sqrt{\sum_{m=1}^{M}\sum_{t=1}^{T}\|z_t^m - \tilde{z}_t^m\|^2}\right] \tag{C33}$$

$$\le 2\sigma\sqrt{MT} \cdot \mathbb{E}\left[\sqrt{\sum_{m=1}^{M}\sum_{t=1}^{T}\|z_t^m - \tilde{z}_{t-1}^{m,*}\|^2 + \|z_t^m - \tilde{z}_t^m\|^2}\right] \tag{C34}$$

$$= 2\sigma\sqrt{MT} \cdot \mathbb{E}\left[\sqrt{\sum_{m=1}^{M}\sum_{t=1}^{T}5 \cdot (\eta_t^m)^2 (Z_t^m)^2}\right] \tag{C35}$$

$$= 2\sqrt{5} \cdot \sigma\sqrt{MT} \cdot D\alpha \cdot \mathbb{E}\left[\sqrt{\sum_{m=1}^{M}\sum_{t=1}^{T}\frac{(Z_t^m)^2}{G_0^2 + \sum_{\tau=1}^{t-1}(Z_\tau^m)^2}}\right] \tag{C36}$$

$$\le 6 \cdot \sigma\sqrt{MT} \cdot D\alpha \cdot \mathbb{E}\left[\sqrt{\sum_{m=1}^{M}\left(6\gamma^2 + 2\log\left(\frac{G_0^2 + \sum_{t=1}^{T-1}(Z_t^m)^2}{G_0^2}\right)\right)}\right] \quad \text{(Lemma 6)}$$

$$\le 6\sigma\sqrt{MT} \cdot D\alpha \cdot \sqrt{M(6\gamma^2 + 2\log(1+\gamma^2 T))}. \tag{C37}$$

By our choice of α, we have $\mathbb{E}[V] = \tilde{O}(\gamma\sigma D\sqrt{MT})$.

Continuing Eq. (C43), we have

$$\begin{aligned} &TM \cdot \mathbb{E}[\mathrm{DualGap}(\bar{z})] \\ &\le O\Big(\gamma\sigma D\sqrt{MT}\Big) + 2\gamma MDG/\alpha + \mathbb{E}[\mathcal{A} + \mathcal{C}_{\mathrm{head}} + (-\mathcal{B}_{\mathrm{tail}} + \mathcal{C}_{\mathrm{tail}}) + V] \\ &= \tilde{O}\Big(\gamma\sigma D\sqrt{MT} + \underbrace{\gamma DM^{3/2}G + DM^{3/2}\mathcal{V}_m(T)}_{\mathcal{A}} + \underbrace{\gamma^2 LD^2}_{\mathcal{C}_{\mathrm{head}}} + \underbrace{\gamma\sigma D\sqrt{MT}}_{V}\Big). \end{aligned}$$

This finishes the proof of Theorem 2.

□

Remark 6 (Getting rid of $\mathcal{V}_1(T)$) We could also use the free parameters α (base learning rate) and obtain the following near linear speed-up result.

Theorem 5 (Smooth Case, free of $\mathcal{V}_1(T)$) *Assume 1, 2, 3 and 4. Let σ, D, G, L be defined therein. For any $\epsilon \in (0, \frac{1}{2})$, let $\bar{z} = \mathrm{LocalAdaSEG}(G_0, D;\ K, M, R;\ T^\epsilon/\sqrt{M})$.*

If $T \geq M^{1/(2\epsilon)}$*, then*

$$\mathbb{E}[\text{DualGap}(\bar{z})] = \tilde{O}\left(\frac{\sigma D}{\sqrt{MT^{1-2\epsilon}}} + \frac{\gamma^2 L D^2}{T^{1-2\epsilon}} + \frac{LD^2 M}{T} + \frac{\gamma G D M^{3/2}}{T^{1+\epsilon}}\right),$$

where $\tilde{O}$ *hides absolute constants, logarithmic factors of problem parameters and logarithmic factors of* T*.*

Proof of Theorem 5 We decompose the term II in Eq.(C5) in a different way. Recall in Step 3 we have shown for all $z \in \mathcal{Z}$, $II(z) \leq \sum_{m=1}^{M} \frac{D^2}{\eta_1^m} + \frac{D^2}{\eta_T^m}$. For the second term, for fixed $m \in [M]$,

$$\sum_{m=1}^{M} D^2/\eta_T^m = \sum_{m=1}^{M} \frac{D}{\alpha}\sqrt{G_0^2 + \sum_{t=1}^{T-1}(Z_t^m)^2} \tag{C38}$$

$$\leq \sum_{m=1}^{M} \frac{D}{\alpha}\left(G_0 + \sum_{t=1}^{T} \frac{(Z_t^m)^2}{\sqrt{G_0^2 + \sum_{\tau=1}^{t-1}(Z_\tau^m)^2}}\right) \qquad \text{(Lemma 7)}$$

$$= \frac{MDG_0}{\alpha} + \sum_{m=1}^{M}\sum_{t=1}^{T} \frac{1}{\alpha^2}(\eta_t^m)^2 (Z_t^m)^2 \tag{C39}$$

$$\leq \frac{\gamma MDG}{\alpha} + \underbrace{\sum_{m=1}^{M}\sum_{t=1}^{\tau_m^*} \frac{1}{\alpha^2}(\eta_t^m)^2 (Z_t^m)^2}_{:=\mathcal{A}_{\text{head}}} + \underbrace{\sum_{m=1}^{M}\sum_{t=\tau_m^*+1}^{T} \frac{1}{\alpha^2}(\eta_t^m)^2 (Z_t^m)^2}_{:=\mathcal{A}_{\text{tail}}} \tag{C40}$$

So we have $\mathbb{E}[\sup_z II(z)] \leq 2\gamma MDG/\alpha + \mathbb{E}[\mathcal{A}_{\text{head}} + \mathcal{A}_{\text{tail}}]$. Then, following the proof in the smooth case, we have

$$TM \cdot \mathbb{E}[\text{DualGap}(\bar{z})] \leq \mathbb{E}[\sup_z \{I(z) + II(z) + III + IV\}] \tag{C41}$$

$$\leq O\left(\gamma\sigma D\sqrt{MT}\right) + 2\gamma MDG/\alpha \tag{C42}$$

$$+ \mathbb{E}[\mathcal{A}_{\text{head}} + \mathcal{C}_{\text{head}} + (\mathcal{A}_{\text{tail}} - \mathcal{B}_{\text{tail}} + \mathcal{C}_{\text{tail}}) + V]. \tag{C43}$$

Recall our choice of $\alpha = T^\epsilon/\sqrt{M}$.
Show $\mathbb{E}[\mathcal{A}_{\text{head}}] = \tilde{O}(1)$. Recall its definition in Eq. (C40).

$$\mathcal{A}_{\text{head}} := \sum_{m=1}^{M}\sum_{t=1}^{\tau_m^*} \frac{1}{\alpha^2}(\eta_t^m)^2 (Z_t^m)^2$$

$$= \frac{D}{\alpha}\sum_{m=1}^{M}\sum_{t=1}^{\tau_m^*} \frac{(Z_t^m)^2}{\sqrt{G_0^2 + \sum_{\tau=1}^{t-1}(Z_\tau^m)^2}}$$

$$\leq \frac{D}{\alpha}\sum_{m=1}^{M}\left(5\gamma G + 3\sqrt{G_0^2 + \sum_{t=1}^{\tau_m^*-1}(Z_t^m)^2}\right) \qquad \text{(Lemma 7)}$$

$$= \frac{D}{\alpha}\sum_{m=1}^{M}\left(5\gamma G + \frac{3D\alpha}{\eta_{\tau_m^*}^m}\right)$$

$$\leq \frac{D}{\alpha}\sum_{m=1}^{M}\Big(5\gamma G + 6\alpha LD\Big) = \frac{5\gamma GDM}{\alpha} + 6LD^2M.$$

By our choice of α we have $\mathbb{E}[\mathcal{A}_{\text{head}}] \leq 5\gamma GDM^{3/2}T^{-\epsilon} + 6LD^2M$.

For $\mathcal{C}_{\text{head}}$ defined in Eq. (C22), following Eq (C29), we have $\mathbb{E}[\mathcal{C}_{\text{head}}] = \tilde{O}(\gamma^2 LD^2T^{2\epsilon})$.

Show $\mathcal{A}_{\text{tail}} + \mathcal{C}_{\text{tail}} - \mathcal{B}_{\text{tail}} \leq 0$. Recall $\mathcal{B}_{\text{tail}}$ is defined in Eq. (C16). By definition,

$$\mathcal{A}_{\text{tail}} + \mathcal{C}_{\text{tail}} - \mathcal{B}_{\text{tail}} = \sum_{m=1}^{M}\sum_{t=\tau_m^*+1}^{T}\Big(\frac{1}{\alpha^2} + \frac{5L}{2}\eta_t^m - \frac{5}{2}\Big)\eta_t^m(Z_t^m)^2.$$

We show $\frac{1}{\alpha^2} + \frac{5L}{2}\eta_t^m - \frac{5}{2} \leq 0$ for all $t \in [T], m \in [M]$. Note that

$$T \geq M^{1/(2\epsilon)} \implies \alpha^2 = (T^\epsilon/\sqrt{M})^2 \geq 1,$$

and that for all $t \geq \tau_m^* + 1$ we have $\eta_t^m \leq 1/(2L)$. And so $\frac{1}{\alpha^2} + \frac{5L}{2}\eta_t^m - \frac{5}{2} \leq 1 + (5/4) - (5/2) = -1/4$. Summarizing, we have shown $\mathcal{A}_{\text{tail}} + \mathcal{C}_{\text{tail}} - \mathcal{B}_{\text{tail}} \leq 0$.

For V defined in Eq. (C19), following Eq. (C37), $\mathbb{E}[V] = \tilde{O}(\gamma\sigma D\sqrt{MT^{1+2\epsilon}})$.

Putting together we have

$$\begin{aligned}
&TM \cdot \mathbb{E}[\text{DualGap}(\bar{z})] \\
&\leq O\Big(\gamma\sigma D\sqrt{MT}\Big) + 2\gamma MDG/\alpha + \mathbb{E}[\mathcal{A}_{\text{head}} + \mathcal{C}_{\text{head}} + (\mathcal{A}_{\text{tail}} - \mathcal{B}_{\text{tail}} + \mathcal{C}_{\text{tail}}) + V] \\
&= \tilde{O}\Big(\gamma\sigma D\sqrt{MT} + \underbrace{\gamma GDM^{3/2}T^{-\epsilon} + LD^2M}_{\mathcal{A}_{\text{head}}} + \underbrace{\gamma^2 LD^2T^{2\epsilon}}_{\mathcal{C}_{\text{head}}} + \underbrace{\gamma\sigma D\sqrt{MT^{1+2\epsilon}}}_{V}\Big).
\end{aligned}$$

This finishes the proof of Theorem 5 □

Appendix D Helper Lemmas

Lemma 6 For any non-negative real numbers $a_1, \ldots, a_n \in [0, a]$, and $a_0 > 0$, it holds

$$\sum_{i=1}^{n}\frac{a_i}{a_0 + \sum_{j=1}^{i-1}a_j} \leq 2 + \frac{4a}{a_0} + 2\log\Big(1 + \sum_{i=1}^{n-1}a_i/a_0\Big).$$

Proof of Lemma 6 See Lemma A.2 of [6].

□

Lemma 7 For any non-negative numbers $a_1, \ldots, a_n \in [0, a]$, and $a_0 > 0$, it holds

$$\sqrt{a_0 + \sum_{i=1}^{n-1}a_i} - \sqrt{a_0} \leq \sum_{i=1}^{n}\frac{a_i}{\sqrt{a_0 + \sum_{j=1}^{i-1}a_j}} \leq \frac{2a}{a_0} + 3\sqrt{a} + 3\sqrt{a_0 + \sum_{i=1}^{n-1}a_i}.$$

Proof of Lemma 6 See Lemma A.1 of [6].

□

Lemma 8 9 For any sequence $\{z_t\}_{t=1}^T \subset \mathcal{Z}^o$, let $\bar{z}$ denote its mean. It holds

$$T \cdot \text{DualGap}(\bar{z}) \leq \sup_{z\in\mathcal{Z}}\sum_{t=1}^{T}\big\langle z_t - z, G(z_t)\big\rangle.$$

Proof of Lemma 8 This lemma depends on the convexity-concavity of the saddle function F.

Denote $\bar{z} := [\bar{x}, \bar{y}]$, $z_t := [x_t, y_t]$. Note $\bar{x} = (1/T)\sum_{t=1}^{T} x_t$ and $\bar{y} = (1/T)\sum_{t=1}^{T} y_t$. By definition of the duality gap and the convexity-concavity of F,

$$\begin{aligned}\text{DualGap}(\bar{z}) &:= \sup_{x\in\mathcal{X}, y\in\mathcal{Y}} F(\bar{x}, y) - F(x, \bar{y}) \\ &\leq \sup_{x\in\mathcal{X}, y\in\mathcal{Y}} \frac{1}{T}\sum_{t=1}^{T} F(x_t, y) - \frac{1}{T}\sum_{t=1}^{T} F(x, y_t).\end{aligned}$$

Let $G(z_t) = G(x_t, y_t) := [d_{x,t}, -d_{y,t}]$. Since $d_{x,t} \in \partial_x F(x_t, y_t)$, for all $x \in \mathcal{X}$ and $y \in \mathcal{Y}$,

$$F(x_t, y) + \langle d_{x,t}, x - x_t\rangle \leq F(x, y).$$

Similarly, for all $x \in \mathcal{X}$ and $y \in \mathcal{Y}$, it holds

$$F(x, y_t) + \langle d_{y,t}, y - y_t\rangle \geq F(x, y).$$

We have

$$\begin{aligned}T \cdot \text{DualGap}(\bar{z}) &\leq \sup_{x\in\mathcal{X}, y\in\mathcal{Y}} \sum_{t=1}^{T} \langle d_{x,t}, x_t - x\rangle - \langle d_{y,t}, y_t - y\rangle \\ &= \sup_{z\in\mathcal{Z}} \sum_{t=1}^{T} \langle G(z_t), z_t - z\rangle.\end{aligned}$$

This completes the proof of Lemma 8. □

Appendix E Additional Experiments

We implement our algorithm and conduct all the experiments on a computer with Intel Core i5 CPU @ 3.20GHz cores, 8GB RAM, and GPU @ GeForce RTX 3090. The deep learning framework we use is PyTorch 1.8.1. The OS environment was created by Conda over Ubuntu 20.04. We use Python 3.7. Python library requirement is specified in the configuration file provided in the supplemental materials. Due to the hardware limitation, we simulate the distributed environment by creating object instances to simulate multiple clients and a central server on one GPU card.

E.1 Stochastic bilinear minimax problem

Experimentally, to validate the performance of our proposed method, we conduct an asynchronous variant of our proposed LocalAdaSEG for the stochastic bilinear minimax problem. Specifically, we vary the number of local iterations K in M workers, where $M = 4$ and the noise level $\sigma = 0.1$. In the case of 'Asynch-50', the local iteration K is in the range of $\{50, 45, 40, 35\}$ for each worker, and $K = 50$ is adopted for all workers in 'Synch-50'. Similarly, in the case of 'Asynch-100', the local iteration K varies in the range of $\{100, 90, 80, 70\}$. In the comparison, K is fixed to 100 for each worker in the case of 'Synch-100'. As can be seen from Fig. E1 (a), both asynchronous and synchronous cases converge to an optimal point after several communication

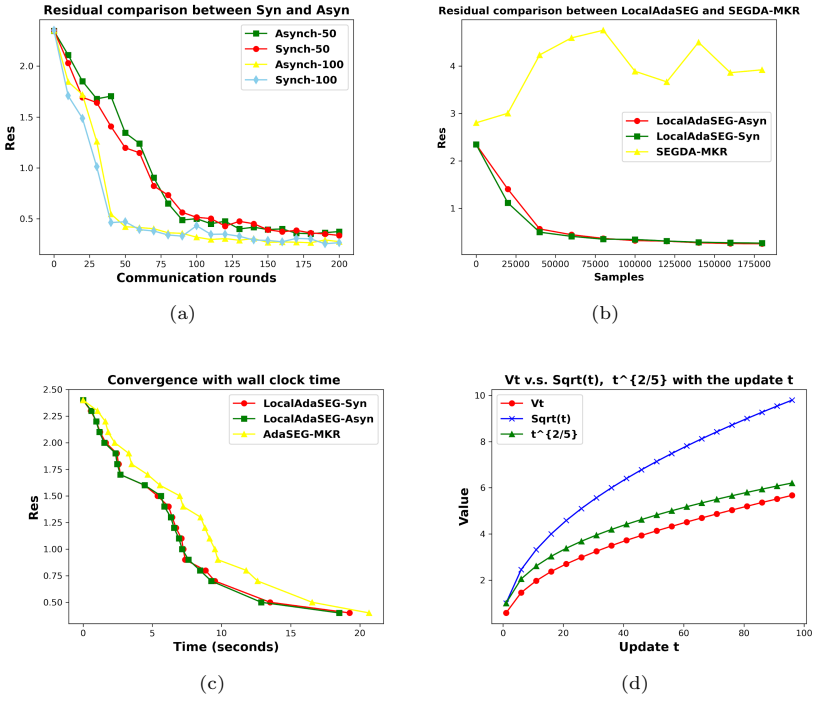


Fig. E1 (a) Residual comparison between synchronous and asynchronous cases with the communication rounds; (b) Residual comparison between LocalAdaSEG (Asynchronous and Synchronous version) and SEGDA-MKR with samples; (c) Residual comparison between LocalAdaSEG (Asynchronous and Synchronous version) and SEGDA-MKR with wallclock time; (d) Comparison of V_t, $\sqrt{t}$, $t^{2/5}$ with the update t.

rounds. Compared with synchronous cases, asynchronicity only affects the convergence rate that is slower than the synchronous version with respect to the communication rounds.

Secondly, we compared our LocalAdaSEG (both Asynchronous and Synchronous versions) with SEGDA of MKR iterations to solve bilinear minimax problems(refer to Section 6.1). Specifically, we choose $M = 4$ workers, the noise level $\sigma = 0.1$ and local iteration $K = 50$ in the Synchronous case, and K in the range of $\{50, 45, 40, 35, 30\}$ in the Asynchronous case. To provide fairness, we run vanilla SEGDA with $M \times K \times R$ iterations on one worker with batchsize $= 1$, where M denotes the number of workers, K denotes the number of local iterations and R represents the number of rounds. The experimental results are illustrated in Fig. E1 (b). As can be seen, the performance of SEGDA is unstable and worse than that of LocalAdaSEG (Asyn. and Syn.). The reason is possible since the batchsize of stochastic gradient $bs = 1$ in each iteration results in a large variance of stochastic gradient estimation. Because there are several workers involved in the optimization in LocalAdaSEG, it has much

more samples in each iteration than that of SEGDA-MKR. It indicates that the stochastic variance is smaller than that of SEGDA-MKR, resulting in the stable performance of LocalAdaSEG.

Thirdly, we also conduct experiments to validate the performance from the aspect of wallclock time on a bilinear minimax problem, where the number of workers $M = 4$, and the noise level $\sigma = 0.1$. We record the wallclock time of reaching the target residual value for synchronous LocalAdaSEG ($K = 50$), the asynchronous version (K in the range of $\{50, 45, 40, 35, 30\}$), and the single thread version. The results are illustrated in Fig. E1 (c). As can be seen, compared with the single thread version, our proposed method speed-ups the convergence. With respect to the wall clock time, Asynchronous LocalAdaSEG(LocalAdaSEG-Asyn) is slightly better than synchronous LocalAdaSEG(synchronous LocalAdaSEG-Syn). Since the tested bilinear minimax problem with noise level $\sigma = 0.1$ is very simple (time cost is around 20 seconds), the differences in time cost between synchronous and asynchronous cases are not significant.

Fourthly, we conduct the experiments with the bilinear case to evaluate the quantity of Vt with the update t. Here, we adopt the same experimental settings as that of experiments in Section 6.1. The noise level $\sigma = 0.1$ and the number of workers $M = 4$. As can be seen from Fig. E1 (d), Vt is really much smaller than the dominant variance term.

E.2 Wasserstein GAN

Inspired by game theory, generative adversarial networks (GANs) have shown great performance in many generative tasks to replicate the real-world rich content, such as images, texts, and music. GANs are composed of two models, a generator and a discriminator, which are competing with each other to improve the performance of a specific task. In this experiment, we aim to train a digit image generator using the MNIST dataset.

It is challenging to train a GAN model due to the slow convergence speed, instability of training or even failure to converge. [2, 3] proposed to use the Wasserstein distance as the GAN loss function to provide stable and fast training. To enforce the Lipschitz constraint on the discriminator, we adopt WGAN with gradient penalty as our experimental model. The objective can be described as

$$\min_G \max_D \left\{ \mathop{\mathbb{E}}_{x\sim\mathbb{P}_r}[D(x)] - \mathop{\mathbb{E}}_{z\sim\mathbb{P}_z}\big[D\big(G(z)\big)\big] - \lambda\big[\big(\|\nabla_{\hat{x}} D(\hat{x})\|_2 - 1\big)^2\big] \right\}, \quad \text{(E44)}$$

where D and G denote the generator and discriminator, $\mathbb{P}_r$ is the data distribution, and $\mathbb{P}_z$ represents the noise distribution (uniform or Gaussian distribution). The point $\hat{x} \sim \mathbb{P}_{\hat{x}}$ is sampled uniformly along straight lines between pairs of points sampled from the real data distribution $\mathbb{P}_r$ and the generator distribution $\mathbb{P}_{\tilde{x}}$, expressed as $\hat{x} := \epsilon x + (1 - \epsilon)\tilde{x}$, where $\epsilon \sim U[0, 1]$.

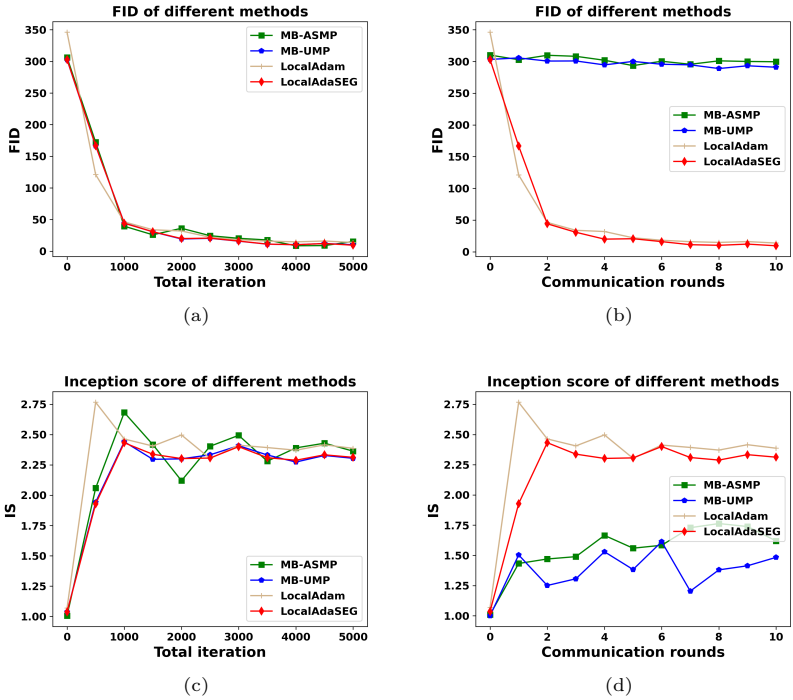


Fig. E2 Subfigures (a)-(b) and (c)-(d) show the results of WGAN trained with LocalAdaSEG and existing optimizers. We plot FID and IS against the number of iterations and communications, respectively.

DCGAN. We implement WGAN with the DCGAN architecture, which improves the original GAN with convolutional layers. Specifically, the generator consists of 3 blocks, which contain deconvolutional layers, batch normalization and activations. The details of the whole generator can be represented as sequential layers {*Linear, BN, ReLU, DeConv, BN, ReLU, DeConv, BN, ReLU, DeConv, Tanh*}, where *Linear*, *BN*, *DeConv* denote the linear, batch normalization and deconvolutional layer, respectively. *ReLU* and *Tanh* represent the activation functions. Similarly, the discriminator also contains 3 blocks, which can be described as sequential layers {*Conv, LReLU, Conv, LReLU, Conv, LReLU, Linear*}, where *Conv* and *LReLU* denote the convolutional layer and Leaky-ReLU activation function, respectively.

Inception score (IS). Inception score (IS) is proposed to evaluate the performance of a GAN with an inception model. IS measures GAN from two aspects simultaneously. Firstly, GAN should output a high diversity of images. Secondly, the generated images should contain clear objects. Specifically, we feed the generated images x into a well-trained inception model to obtain the

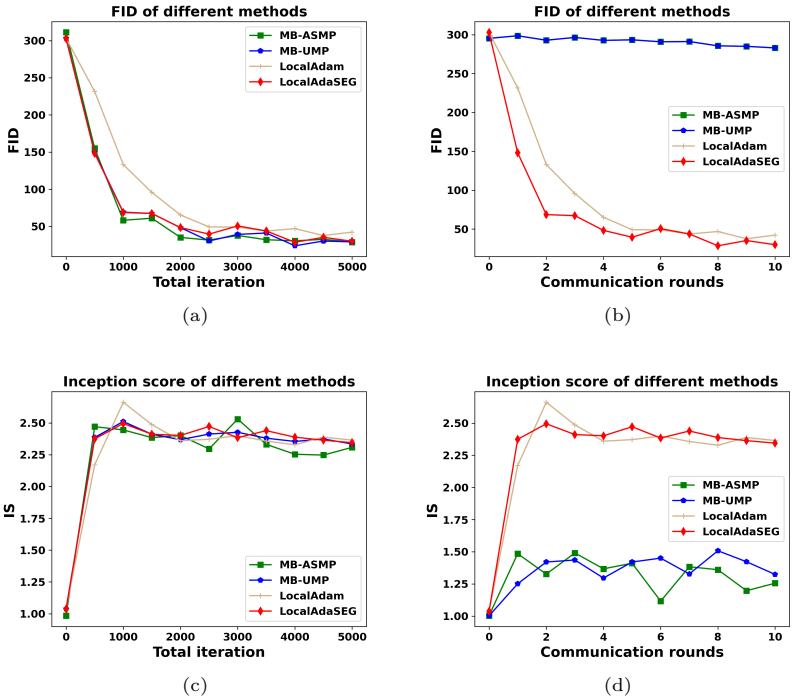


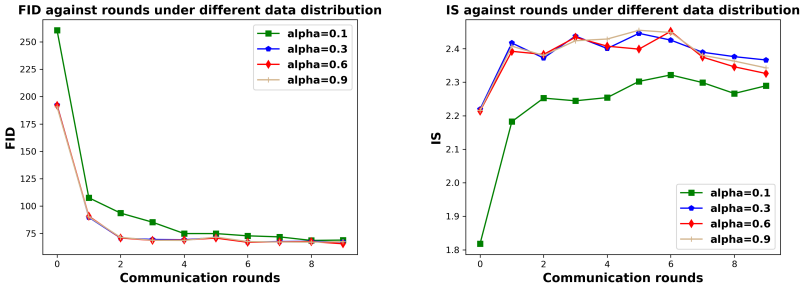
Fig. E3 Subfigures (a)-(b) and (c)-(d) show the results of Federated WGAN trained with LocalAdaSEG and existing optimizers. We plot FID and IS against the number of iterations and communications, respectively.

output y. Then, IS can be calculated by the following equation:

$$\mathrm{IS} := \exp\left(\mathop{\mathbb{E}}_{x\sim\mathbb{P}_g}\left[D_{\mathrm{KL}}\big(p(y\,|\,x)\|p(y)\big)\right]\right), \tag{E45}$$

where $\mathbb{P}_g$ is the generator model distribution. Essentially, IS computes the mutual information $I(y;\ x) = H(y) - H(y\,|\,x)$, where $H(\cdot)$ denotes the entropy. The larger $H(y)$, the more diversity in the generated images. The lower $H(y\,|\,x)$ implies the input x belongs to one class with a higher probability. In summary, IS is bounded by $1 \leq \mathrm{IS} \leq 1000$. The higher IS implies a better performance of a GAN.

Fréchet Inception Distance (FID). Although IS can measure the diversity and quality of the generated images, it still has some limitations, such as losing sight of the true data distribution, failure to measure the model generalization. FID is an improved metric for GAN, which cooperates with the training samples and generated samples to measure the performance together. Specifically, we feed the generated samples and training samples into an inception model to extract the feature vectors, respectively. Usually, we extract the logits value before the last sigmoid activation as the feature vector with



(a) (b)

Fig. E4 Subfigures (a)-(b) show the FID and IS against communication rounds of WGAN trained over MNIST dataset under different Dirichlet distribution.

dimension 2048. Essentially, FID is the Wasserstein metric between two multidimensional Gaussian distributions: $\mathcal{N}(\mu_g, \Sigma_g)$ the distribution of feature vectors from generated samples and $\mathcal{N}(\mu_r, \Sigma_r)$ the distribution of feature vectors from the training samples. It can be calculated as

$$\text{FID} := \|u_r - u_g\|^2 + \text{tr}\big(\Sigma_r + \Sigma_g - 2(\Sigma_r\Sigma_g)^{1/2}\big) \tag{E46}$$

where $\text{tr}(\cdot)$ denotes the trace of a matrix. The lower the FID, the better the performance of a GAN.

Implementation details. Experiments are conducted on the MNIST datasets of digits from 0 to 9, with 60000 training images of size 28×28. We adopt the same network architecture of WGAN as that of DCGAN [3]. We simulate $M = 4$ parallel workers and run LocalAdaSEG with the batch size 128 and local iteration steps $K = 500$. In the homogeneous setting, the local data in each worker is uniformly sampled from the entire dataset. In the heterogeneous setting, we partition the MNIST dataset into 4 subsets using the partition methods in [38]. Then each worker is loaded with a fraction of the dataset. Due to non-adaptive learning rates, LocalSGDA, LocalSEGDA, and MB-SEGDA are hard to tune and do not achieve satisfactory performance for training WGAN. For a better illustration, we only show the performance of LocalAdaSEG, MB-UMP, MB-ASMP and Local Adam. To measure the efficacy of the compared optimizers, we plot FID and IS [30] against the number of iterations and communications, respectively.

To investigate the convergence rate of LocalAdaSEG under different data distributions, we conduct to train WGAN over MNIST dataset with different Dirichlet distributions. In Fig. E4, it shows the FID and IS of training the WGAN under the Dirichlet distribution with various parameters $\alpha \in \{0.1, 0.3, 0.6, 0.9\}$. It should be noted that when α increases, the data distribution trends closer to the homogeneous setting. As can be seen from Fig. E4, it converges faster when the parameter α decreases.

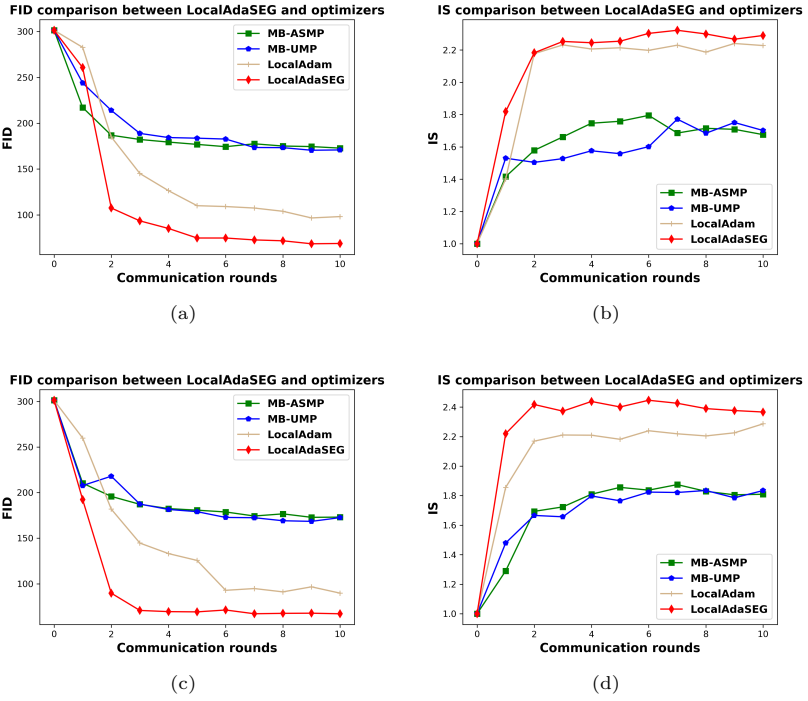
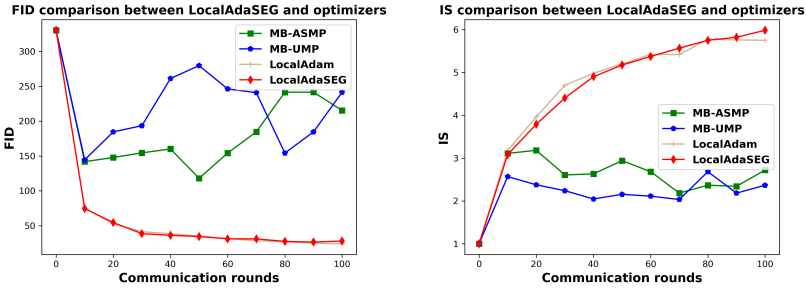


Fig. E5 Subfigures (a)-(b) show the FID and IS against communication rounds of WGAN trained over MNIST dataset with $\alpha = 0.1$; (c)-(d) show the FID and IS against communication rounds of WGAN trained over MNIST dataset with $\alpha = 0.3$.

Furthermore, we also compare LocalAdaSEG with other existing optimizers under various Dirichlet distributions which parameter $\alpha \in \{0.1, 0.3\}$, respectively. As can be seen from Fig. E5, our proposed LocalAdaSEG also achieves a faster convergence compared with exiting minimax optimizers.

E.3 BigGAN on CIFAR10

BigGAN. Although a variety of GANs were investigated to effectively generate images, they are still restricted to small image synthesis and the training process remains dependent on augmentations and hyperparameters. BigGAN is a typical network to pull together a suite of recent best practices in training class-conditional images and scaling up the batch size and number of model parameters. The result is the routine generation of both high-resolution and high-fidelity natural images. Since utilizing the self-attention module and skip connections, BigGAN can not be simply considered as a sequential combination of layers. Here, we only describe the key module in the BigGAN. Specifically, the generator consists of 1 linear layer, N generator blocks, and 1 sequential layer. Each generator block can be represented as several layers $\{BN, ReLU,$



(a) (b)

Fig. E6 Subfigures (a)-(b) show the FID and IS against communication rounds of BigGAN over the CIFAR10 dataset.

SNConv, BN, ReLU, SNConv, SNConv}, where *SNConv* denotes 2d convolutional layer with the spectral norm. Similarly, The discriminator also consists of linear layers and discriminator blocks. Each discriminator block can be listed as several layers {*ReLU, AvgPool, SNConv, SNConv, SNConv*}, where *AvgPool* denotes the average pooling.

CIFAR10. The CIFAR-10 dataset consists of 60000 32x32 color images in 10 classes, with 6000 images per class. There are 50000 training images and 10000 test images. The test batch contains exactly 1000 randomly-selected images from each class. The training batches contain the remaining images in random order, but some training batches may contain more images from one class than another. Between them, the training batches contain exactly 5000 images from each class.

Parameter Setup. We implement the BigGAN with the original CIFAR10 dataset, meaning that all the images are fed into the BigGAN without cropping and rotation. The experiments are conducted among $M = 4$ parallel workers in a heterogeneous setting. It implies that all the training images are divided into 4 parts by using Dirichlet distribution with parameter $\alpha = 0.6$. Each work runs the LocalAdaSEG with the batch size $bs = 125$ and local iteration steps $K = 100$. The input noise dimension is 125, and the channel of the generator block and discriminator is set to 16. To show the performance of LocalAdaSEG, MB-UMP, MB-ASMP, and Local Adam, We plot FID and IS against the communication rounds in the Fig. E6.

Fig. E6 illustrates the FID and IS score of BigGAN over the CIFAR10 dataset. As can be seen that LocalAdaSEG and Local Adam converge faster than other optimizers.